A new model for suspension bridges involving the convexification of the cables

Graziano CRASTA[†] – Alessio FALOCCHI[‡] – Filippo GAZZOLA[‡]

[†]Dipartimento di Matematica "G. Castelnuovo" - Sapienza Università di Roma,
P.le Aldo Moro 5 - 00185 Roma, Italy

[‡]Dipartimento di Matematica - Politecnico di Milano,
Piazza Leonardo da Vinci 32 - 20133 Milano, Italy

graziano.crasta@uniroma1.it - alessio.falocchi@polimi.it - filippo.gazzola@polimi.it

Abstract

The final purpose of this paper is to show that, by inserting a convexity constraint on the cables of a suspension bridge, the torsional instability of the deck appears at lower energy thresholds. Since this constraint is suggested by the behavior of real cables, this model appears more reliable than the classical ones. Moreover, it has the advantage to reduce to two the number of degrees of freedom (DOF), avoiding to introduce the slackening mechanism of the hangers. The drawback is that the resulting energy functional is extremely complicated, involving the convexification of unknown functions. This paper is divided in two main parts. The first part is devoted to the study of these functionals, through classical methods of calculus of variations. The second part applies this study to the suspension bridge model with convexified cables.

Keywords: suspension bridges, instability, convexification.

AMS Subject Classification (MSC2010): 35C31, 74B20.

Contents

1 Introduction and the physical model

A suspension bridge is composed by four towers, a rectangular deck, two sustaining cables and a large number of hangers. In Figure 1 we sketch the side view of a bridge where we insert a reference system (O, x, y) in which the vertical displacement w is positive if directed downwards while x is oriented horizontally along the deck. We model the portion of the deck between the towers as a degenerate plate

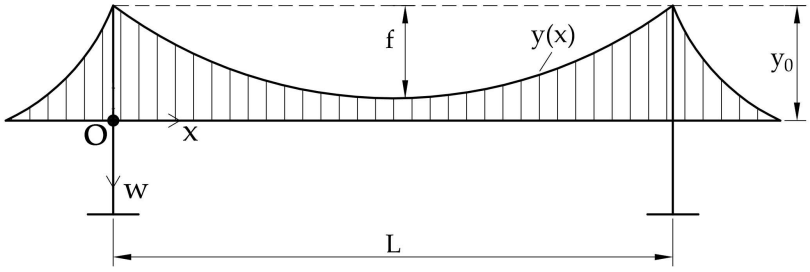

Figure 1: Sketch of the side view of a suspension bridge.

occupying at rest the planar position $(0, L) \times (-\ell, \ell) \subset \mathbb{R}^2$, composed by a central beam of length L in its midline and cross sections of length $2\ell \ll L$ whose midpoints lie on the beam. Each cross section is free to rotate around the beam and to leave the horizontal equilibrium position. The hangers link the endpoints of the cross sections (the longer edges of the degenerate plate) to the cables. This model is called *fish-bone* in [6] and a preliminary linear version of it was suggested in [30, p.458, Chapter VI].

The elastic deformation of the hangers is usually neglected in the engineering literature, see e.g. [23], this simplification being only partially justified by precise studies on linearized models. The hangers are considered as rigid bars so that the deck and the cables undergo the same movement. Nevertheless this assumption is unreasonable since the hangers resist to traction but not to compression. Slackening of the hangers was observed by Farquharson [1, V-12] during the Tacoma Narrows Bridge (TNB) collapse: *one of the four suspenders in its group was permanently slack*. In the simplified model with rigid hangers considered in [17], the cable displayed shapes similar to those depicted in Figure 2. These

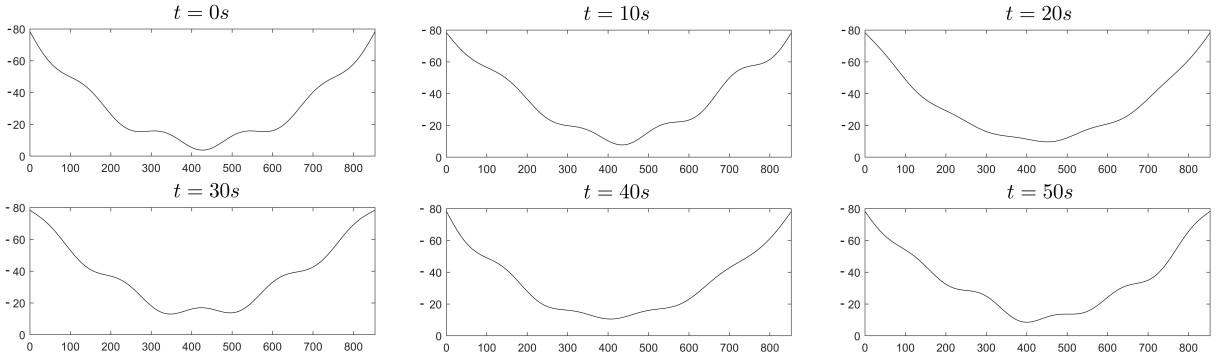

Figure 2: In case of rigid hangers, cable shape with the deck oscillating on the 9th longitudinal mode of initial amplitude 3.87m, see [17].

pictures reproduce the shape every 10s on $[0, L]$ (with $L = 853.44$m as for the TNB). The nonconvex shape becomes more and more evident if the energy in the system (the amplitude of oscillation) is increased. For the plots in Figure 2 the oscillating mode of the deck is the 9th and the initial amplitude is 3.87m, which lies in a physical range. Therefore, the assumption of undeformable rigid hangers leads to unrealistic shapes: in real bridges, the cables never take this shape due to their mass and because, instead of the cables losing convexity, the slackening of the hangers occurs. Moreover, a nonconvex

configuration would increase the energy and the tension of the cable, against the variational principle of minimization of the energy. For these reasons, as in [20] we assume here that the actual shape of the cables coincides with its *convexified shape*, namely the shape minimizing its length at the same loading condition. Acting only on this geometric feature, we are able to propose a model with only two DOF in which the slackening of the hangers is considered indirectly. The great advantage is that we do not need to find a nonlinearity simulating the slackening mechanisms.

The drawback is that the convexity constraint leads to some technical mathematical difficulties, see [9, 10]. This is why Section 2 is fully devoted to state some general results related to the convexification of one dimensional functions. In Theorem 2.8 we compute the variation of functionals containing a convexification. This characterization is new and, in our opinion, of independent interest with possible applications to more general variational problems. The convexification makes the energy function non-differentiable: its variation yields a weak form of a *system of partial differential inclusions* (see (4.2) in Section 4.2) for which the uniqueness of the solution is not expected. However, by exploiting the peculiarity of the model, we are able to show that Galerkin approximation of the problem admits a unique classical solution, because the obstruction to the differentiability of the energy is ruled out in a finite dimensional phase space. This suggests to introduce the class of *approximable solutions* of the problem, namely solutions that are the limit of the Galerkin subsequences, see Definition 4.4 in Section 4.2. This class of solutions will be physically justified and it will be shown that they are representative of the full problem; moreover, within this class we are able to obtain existence results, see Theorem 4.5. This requires some particular attention due to the convexification and to the unusual behavior of test functions.

The torsional oscillations of the deck were the main cause for the TNB collapse [1] and of several other collapses, see e.g. [19]. A new mathematical explanation for the origin of torsional oscillations was given in [2] through the introduction of suitable Poincaré maps: these oscillations appear whenever there is a large amount of energy within the bridge and this happens due to the nonlinear behavior of structures. The model in [2] was fairly simplified, but the very same conclusion was subsequently reached in more sophisticated models [3, 4, 6, 11, 16, 17]. A further purpose of the paper is to study the torsional instability of the deck through the model with convexified cables. To this end, we proceed numerically by introducing a new algorithm dealing with the convexification at the beginning of each temporal iteration. We then numerically show that the slackening mechanism hidden in the convexification of the cables yields energy thresholds of instability for high modes significantly smaller than in models where slackening is neglected. This means that *the slackening of the hangers must be taken into account because it gives lower thresholds of torsional instability.*

This paper is organized as follows. In Section 2 we recall some features of the convexification of a function: we focus on the particular situation that applies to a cable since the general setting may be fairly complicated. In Section 3 we complete the analysis of the model through a careful energy balance. This enables us to derive the differential inclusions and, then, the differential equations related to approximable solutions in Section 4. In Section 5 we report on our numerical experiments and results. Sections 6 and 7 are devoted to the proofs of our results. Finally, in Section 8 we quickly outline the conclusions.

Throughout this paper we denote the derivatives of a function $f = f(t)$ (depending only on t), of a function $g = g(x)$ (depending only on x) and the partial derivatives of a function $w = w(x,t)$, respectively by

$$\dot{f} = \frac{df}{dt}, \qquad g' = \frac{dg}{dx}, \qquad w_x = \frac{\partial w}{\partial x}, \quad w_t = \frac{\partial w}{\partial t},$$

and similarly for higher order derivatives.

2 The convexification of one-dimensional smooth functions

2.1 A possible procedure to find f^{**}

Let $\mathcal{I} = (a, b) \subset \mathbb{R}$ be an open bounded interval. Since we are interested in the specific application of a *real physical* cable, whose shape is described by a function in $H^2(\mathcal{I}) \subset C^1(\overline{\mathcal{I}})$, we consider functions

$$f \in C^1(\overline{\mathcal{I}}) \tag{2.1}$$

avoiding more general assumptions on f. Thanks to (2.1) the existence of a tangent line for all $x \in \overline{\mathcal{I}}$ is ensured.

The convexification of a function can be defined in several different equivalent ways, see [15]. Here we start with the following.

Definition 2.1. *Given f satisfying (2.1), its convexification $f^{**}(x)$ is the largest convex function everywhere less than or equal to $f(x)$. Hence,*

$$f^{**}(x) \le f(x), \qquad f^{**}(x) \ge f^{**}(\overline{x}) + f^{**\prime}(\overline{x})(x - \overline{x}) \qquad \forall x, \overline{x} \in \overline{\mathcal{I}}, \tag{2.2}$$

and $f^{**}(x)$ is the largest convex function satisfying (2.2).

If f is globally convex, then $f = f^{**}$ in $\overline{\mathcal{I}}$, and the graph of f lies above the tangent line in each point $\big(\overline{x}, f(\overline{x})\big)$, namely

$$f(x) \ge f(\overline{x}) + f'(\overline{x})(x - \overline{x}) \qquad \forall x, \overline{x} \in \mathcal{I}. \tag{2.3}$$

If $f \neq f^{**}$, inequality (2.3) suggests a simple way to obtain its convexification. Denote by N the set of the points $\overline{x} \in \mathcal{I}$ such that (2.3) is not verified for some $x \in \mathcal{I}$. Due to the continuity of f and f', see (2.1), the set N is open and is composed by a number of disjoint open maximal nonempty intervals, that we denote by I^i with i varying in some possibly infinite set of integers $J := \{1, 2, \dots\}$:

$$N = \{\overline{x} \in \mathcal{I} : \exists x \in \mathcal{I} \ \ s.t. \ \ f(x) < f(\overline{x}) + f'(\overline{x})(x - \overline{x})\} = \bigcup_{i \in J} I^i.$$

All these intervals are nonempty and delimited by two points that we denote by a^i and b^i:

$$I^i := (a^i, b^i) \subset \mathcal{I} \qquad \forall i \in J.$$

In order to find f^{**}, we replace f on these intervals with linear functions whose graphs link the endpoints $\big(a^i, f(a^i)\big)$ and $\big(b^i, f(b^i)\big)$ for all $i \in J$, namely

$$f^{**}(x) = \begin{cases} f(a^i) + \dfrac{f(b^i) - f(a^i)}{b^i - a^i}(x - a^i) & x \in I^i, \ i \in J, \\ f(x) & x \in \overline{\mathcal{I}} \setminus \bigcup\limits_{i \in J} I^i. \end{cases} \tag{2.4}$$

Note that if $a^i \neq a$ and $b^i \neq b$ for some $i \in J$, see Figure 3 on the left, the graph of the linear function coincides with the tangent lines to f at the endpoints of this interval, that is,

$$\frac{f(b^i) - f(a^i)}{b^i - a^i} = f'(a^i) = f'(b^i). \tag{2.5}$$

If $a^i = a$ or $b^i = b$ for some $i \in J$, then (2.5) holds except at the boundary points, see Figure 3 on the right. In any case, we obtain that $f^{**} \in C^1(\overline{\mathcal{I}})$.

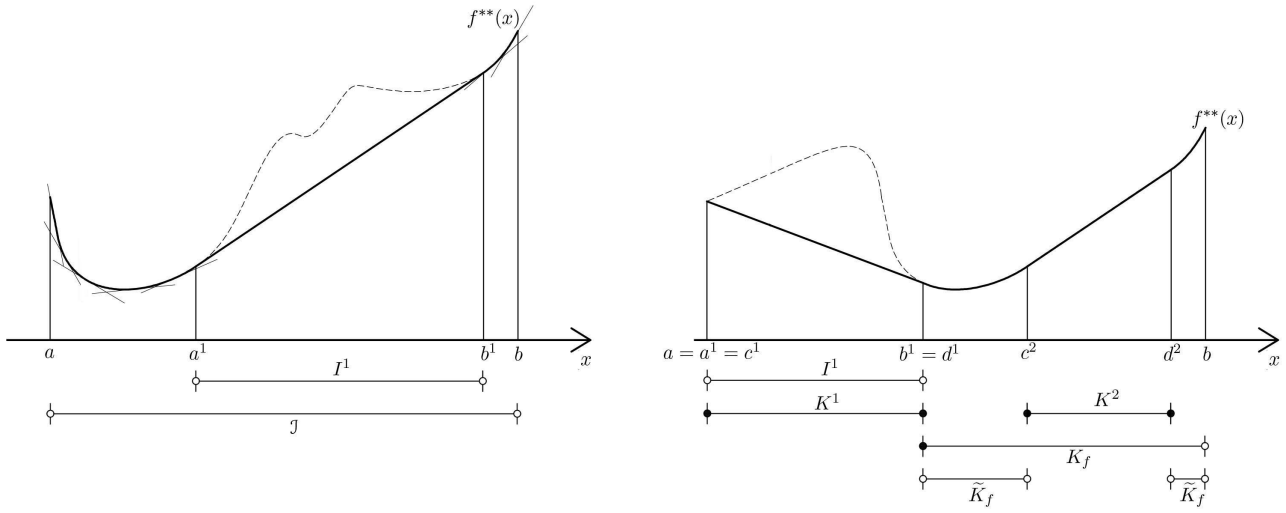

Figure 3: Examples of convexification of f.

In the sequel a major role will be played by the maximal intervals where f^{**} is affine. We denote by $K^i = [c^i, d^i]$, $i \in J_C$, the (possibly countable) family of all these intervals. Let $K_f := \mathcal{I} \setminus N$ be the contact set of f, i.e.

$$K_f := \{x \in \mathcal{I} : \ f(x) = f^{**}(x)\}$$

and note that $c^i, d^i \in K_f \cup \{a, b\}$. We also use the notation

$$\widetilde{K}_f := K_f \setminus \bigcup_{i \in J_C} K^i.$$

Around points $x \in \widetilde{K}_f$ the function f is strictly convex, meaning that

$$f^{**}(x) > f(x_0) + f'(x_0)\,(x - x_0), \qquad \forall x \in [a, b],\ x \neq x_0.$$

More precisely, the set $\{(x, f^{**}(x)) : \ x \in \widetilde{K}_f \cup \{a, b\}\}$ coincides with the set $\operatorname{expo}\operatorname{epi} f^{**}$ of exposed points of the epigraph of f^{**}, see Section 6 for the precise definitions and Figure 3 on the right.

2.2 The variation of functionals of convexified functions

In order to study the behavior of the cables, we need to compute the variation of energies depending on the convexification of a function. We deal with functionals such as $u \mapsto \int_{\mathcal{I}} [\Lambda(u)]^{**} dx$ with $\Lambda \in C^1(\mathbb{R})$ and we need to compute the Gateaux derivative of such functionals. As we shall see, in general these functionals are not Gateaux differentiable at every point. To illustrate this phenomenon, let us consider first the particular case $\Lambda(u) = u$.

Proposition 2.2. *Let $f \in C^1(\bar{\mathcal{I}})$ and let f^{**}, $K^i = [c^i, d^i]$ ($i \in J_C$) and $\widetilde{K}_f$ be as in Section 2.1. Let $\varphi \in C_c^\infty(\mathcal{I})$, and, for every $i \in J_C$, let us define the extended real-valued functions*

$$\varphi_i^{\pm} \colon K^i \to \overline{\mathbb{R}}, \qquad \varphi_i^{\pm}(x) := \begin{cases} \varphi(x) & x \in K^i \cap (K_f \cup \{a, b\}), \\ \pm\infty & x \in K^i \setminus (K_f \cup \{a, b\}). \end{cases} \tag{2.6}$$

Then we have

$$\lim_{s \to 0^{\pm}} \int_{\mathcal{I}} \frac{(f + s\varphi)^{**} - f^{**}}{s}\, dx = \int_{\mathcal{I}} \mathcal{J}_{\pm}^{\varphi}\, dx, \tag{2.7}$$

where

$$\mathcal{J}^{\varphi}_{\pm}(x) := \begin{cases} \pm(\pm\varphi_i^{\pm})^{**}(x) & x \in K^i,\ i \in J_C, \\ \varphi(x) & x \in \widetilde{K}_f. \end{cases} \tag{2.8}$$

The proof of Proposition 2.2 is given in Section 6. As a straightforward consequence of Proposition 2.2, we have

Corollary 2.3. *Under the same assumptions of Proposition 2.2, the functional $f \mapsto \int_{\mathcal{I}} f^{**}$ is Gateaux–differentiable at f if and only if*

$$\overline{K_f} = \overline{\widetilde{K}_f}, \quad \textit{i.e., } f > f^{**} \textit{ on any open interval where } f^{**} \textit{ is affine.} \tag{2.9}$$

In this case, for every $\varphi \in C_c^{\infty}(\mathcal{I})$ it holds that $\mathcal{J}^{\varphi}_{+} = \mathcal{J}^{\varphi}_{-} =: \mathcal{J}^{\varphi}$, with

$$\mathcal{J}^{\varphi}(x) := \begin{cases} \varphi(a^i) + \dfrac{\varphi(b^i) - \varphi(a^i)}{b^i - a^i}(x - a^i) & x \in I^i,\ i \in J, \\ \varphi(x) & x \in K_f. \end{cases} \tag{2.10}$$

Remark 2.4. When condition (2.9) is satisfied, the intervals I^i coincide with the interior of the intervals K^i, i.e. one has that $a^i = c^i$ and $b^i = d^i$ for every $i \in J$, see Figure 3 on the right.

Remark 2.5. Note that if $f \in C^1(\bar{\mathcal{I}})$ and $\varphi \in C_c^{\infty}(\mathcal{I})$ then $\mathcal{J}^{\varphi}_{\pm}, \mathcal{J}^{\varphi} \in W^{1,1}(0, L)$.

Proposition 2.2 states that the shape of the test function φ may not be preserved whenever the variation involving a convexification is concerned, see Figure 4b). Clearly, in the case where f is globally convex the shape of φ is maintained, and we are back to the classical Gateaux derivative. This possible change of φ makes the problem mathematically very challenging and this is the price to pay in order to have a physically reliable modeling of the cables.

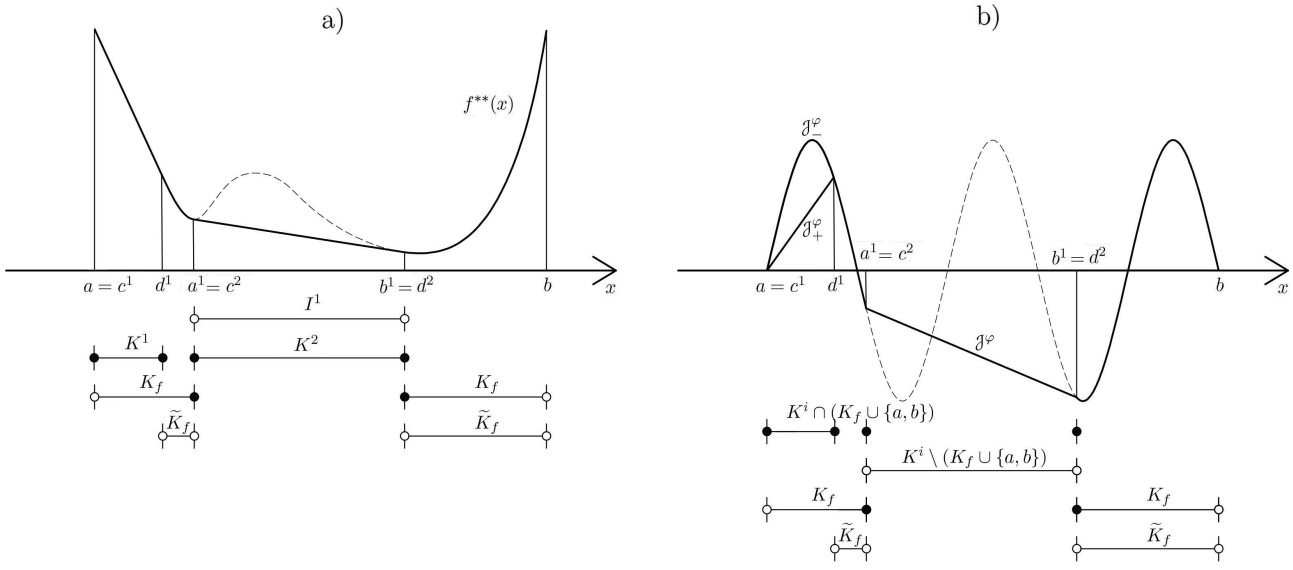

Figure 4: a) Convexification of a function f and b) the corresponding $\mathcal{J}^{\varphi}_{\pm}(x)$, $\mathcal{J}^{\varphi}(x)$ introduced, respectively, in (2.8) and (2.10).

In the following example we explain why assumption (2.9) is necessary in order to have the Gateaux–differentiability of the functional.

Example 2.6. For some $\mu, \nu \in \mathbb{R}$, take $f(x) = \mu x + \upsilon$ on $\mathcal{I} = (-2, 2)$ and take $\varphi \in C_c^\infty(\mathcal{I})$ defined by

$$\varphi(x) = \begin{cases} e^{\frac{1}{x^2-1}} & x \in (-1, 1), \\ 0 & x \in \overline{\mathcal{I}} \setminus (-1, 1). \end{cases}$$

Computing the limits (2.7) we obtain

$$\lim_{s \to 0\pm} \int_{\mathcal{I}} \frac{(s\varphi)^{**}}{s}\, dx = \int_{\mathcal{I}} \pm(\pm\varphi)^{**} dx, \tag{2.11}$$

that depend on the sign of s. Indeed, if $s > 0$ we have $(s\varphi)^{**} \equiv 0$ so that (2.11) vanishes, on the other hand, if $s < 0$, we have that $(s\varphi)^{**} = s[-(-\varphi)^{**}]$, and we obtain the point $\zeta \approx 0.25$, such that

$$-(-\varphi)^{**}(x) = \begin{cases} \varphi(x) & |x| \in [0, \zeta], \\ \dfrac{e^{\frac{1}{\zeta^2-1}}}{\zeta - 2}(|x| - 2) & |x| \in (\zeta, 2), \end{cases}$$

see Figure 5. It is readily seen that the right and left limits of (2.11) are different, implying the

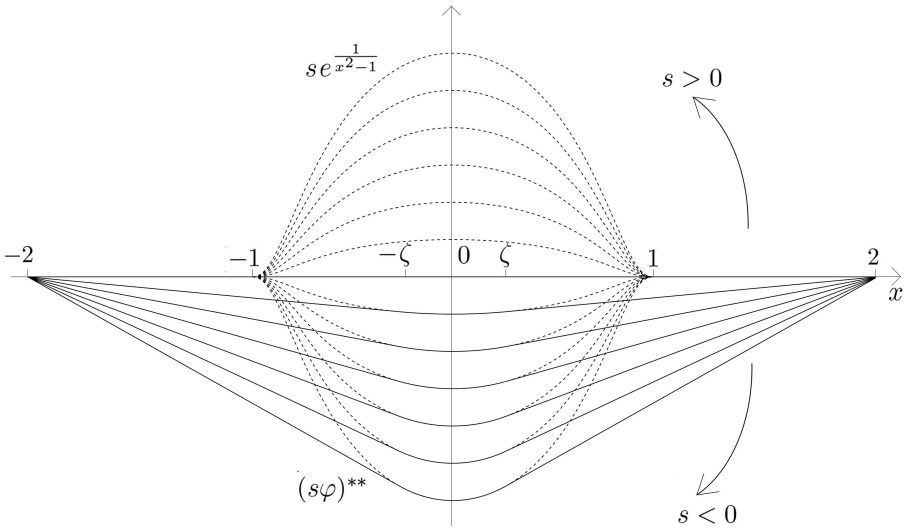

Figure 5: Plot of $(s\varphi)^{**}$ and $s\varphi$ (dashed), for some values of the parameter s.

non-existence of the Gateaux derivative. □

Let us show in a simple case how the functions $\varphi_i^{\pm}$, defined at (2.6), appear in the computation of $\mathcal{J}_{\pm}^{\varphi}$.

Example 2.7. Let $\mathcal{I} = (0, 4\pi)$ and let $f\colon \overline{\mathcal{I}} \to \mathbb{R}$ be the function $f(x) = 1 - \cos x$. Hence, $f \in C^1(\overline{\mathcal{I}})$, $f^{**} \equiv 0$, $K_f = \{2\pi\}$, so that there is only one maximal interval $K^1 := [0, 4\pi]$ where f^{**} is affine. Given $\varphi \in C_c^\infty(\mathcal{I})$, we have that

$$\varphi_1^+(x) = \begin{cases} \varphi(x) & x \in \{0, 2\pi, 4\pi\}, \\ +\infty & \text{otherwise.} \end{cases}$$

Hence $(\varphi_1^+)^{**}$ is the continuous function, affine in $[0, 2\pi]$ and $[2\pi, 4\pi]$, such that $(\varphi_1^+)^{**}(2k\pi) = \varphi(2k\pi)$ for $k = 0, 1, 2$, and $\mathcal{J}_+^{\varphi} = (\varphi_1^+)^{**}$. The function $\mathcal{J}_-^{\varphi}$ can be computed in a similar way. □

The next statement generalizes Proposition 2.2 and provides the main result of this section.

Theorem 2.8. *Consider $u \in C^1(\overline{\mathcal{I}}, \mathbb{R})$, $\Lambda \in C^1(\mathbb{R})$ and let Λ' be its derivative. Let $f := \Lambda \circ u : \overline{\mathcal{I}} \to \mathbb{R}$ and let f^{**}, I^i $(i \in J)$, K^i $(i \in J_C)$ and $\widetilde{K}_f$ be as in Section 2.1. Furthemore, let f satisfy assumption* (2.9). *Then, for all $\varphi \in C_c^\infty(\mathcal{I})$, we have*

$$\lim_{s\to 0} \int_{\mathcal{I}} \frac{[\Lambda(u+s\varphi)]^{**} - [\Lambda(u)]^{**}}{s}\, dx = \int_{\mathcal{I}} \mathcal{G}^{u,\varphi}\, dx,$$

where

$$\mathcal{G}^{u,\varphi}(x) := \begin{cases} \varphi(a^i)\Lambda'\big(u(a^i)\big) + \dfrac{\varphi(b^i)\Lambda'\big(u(b^i)\big) - \varphi(a^i)\Lambda'\big(u(a^i)\big)}{b^i - a^i}(x - a^i) & x \in I^i, \\ \varphi(x)\Lambda'\big(u(x)\big) & x \in \overline{\mathcal{I}} \setminus \bigcup\limits_{i\in J} I^i. \end{cases}$$

Also the proof of Theorem 2.8 is given in Section 6. Here we give an instructive application of Theorem 2.8.

Example 2.9. Take $\theta \in C^1(\overline{\mathcal{I}})$, $\Lambda(\theta) = \sin\theta$ and $\psi \in C_c^\infty(\mathcal{I})$, then Theorem 2.8 yields

$$\lim_{s\to 0} \int_{\mathcal{I}} \frac{[\sin(\theta + s\psi)]^{**} - [\sin\theta]^{**}}{s}\, dx = \int_{\mathcal{I}} \mathcal{G}^{\theta,\psi}\, dx,$$

with

$$\mathcal{G}^{\theta,\psi}(x) := \begin{cases} \psi(a^i)\cos\big(\theta(a^i)\big) + \dfrac{\psi(b^i)\cos\big(\theta(b^i)\big) - \psi(a^i)\cos\big(\theta(a^i)\big)}{b^i - a^i}(x - a^i) & x \in I^i, \\ \psi(x)\cos\big(\theta(x)\big) & x \in \overline{\mathcal{I}} \setminus \bigcup\limits_{i\in J} I^i. \end{cases} \tag{2.12}$$

2.3 Properties of the projection on the cone of convex functions

In this section we give some properties of convexified functions that we will use in the sequel to obtain a priori estimates. In the sequel we denote by $\|\cdot\|_p$ the norm related to the Lebesgue space $L^p(a,b)$ with $1 \le p \le \infty$. All the proofs are given in Section 6.

Proposition 2.10. *Let $T\colon C^0([a,b]) \to C^0([a,b])$ be the operator defined by*

$$Tf := (F^{**})', \qquad \text{where } F(x) := \int_a^x f(y)\, dy, \quad y \in [a,b]. \tag{2.13}$$

Then

$$\int_a^b |Tf - Tg| \le \int_a^b |f - g| \qquad \forall f, g \in C^0([a,b]). \tag{2.14}$$

Proposition 2.10 is essential to show that the map T is Lipschitzian from L^1 to L^1.

Proposition 2.11. *Let $T\colon L^1(a,b) \to L^1(a,b)$ be the operator defined by* (2.13). *Then*

$$\|Tf - Tg\|_1 \le \|f - g\|_1 \qquad \forall f, g \in L^1(a,b). \tag{2.15}$$

In turn, Proposition 2.11 enables us to prove that the convexification is a Lipschitzian transformation from $W_0^{1,1}$ to $W_0^{1,1}$.

Corollary 2.12. *The operator $P\colon W_0^{1,1}(a,b) \to W_0^{1,1}(a,b)$, defined by $P[F] := F^{**}$, is Lipschitz continuous. More precisely,*

$$\|F^{**} - G^{**}\|_{W^{1,1}} \le \left(\frac{b-a}{2} + 1\right) \|F' - G'\|_1 \qquad \forall F, G \in W_0^{1,1}(a,b).$$

In the sequel we use Tg and G in analogy to Tf and F as defined in (2.13); moreover, we denote by $\mathcal{J}_F^\varphi$, $\mathcal{G}^{F,\psi}$ and $\mathcal{J}_G^\varphi$, $\mathcal{G}^{G,\psi}$ the corresponding functions associated respectively to F and G as in (2.10) and (2.12). About the regularity of $\mathcal{J}_F^\varphi$ and $\mathcal{J}_G^\varphi$ we refer to Remark 2.5 and similarly for $\mathcal{G}^{F,\psi}$ and $\mathcal{G}^{G,\psi}$.

The next statement will be crucial to prove the existence and uniqueness result in Section 4.2.

Proposition 2.13. *Let $T\colon L^1(a,b) \to L^1(a,b)$ be the operator defined by* (2.13)*. Then*

$$\left| \int_a^b [Tf\ (\mathcal{J}_F^\varphi)' - Tg\ (\mathcal{J}_G^\varphi)']dx \right| \le \|\varphi'\|_\infty \|f - g\|_1 \qquad \forall f, g \in L^1(a,b),\ \forall \varphi \in C_c^\infty(\mathcal{I}).$$

Similarly, it is possible to state the following more general result.

Proposition 2.14. *Let Λ and $\mathcal{G}^{\theta,\psi}$ be as in Example 2.9, $\mathcal{H} \in \mathrm{Lip}(\mathbb{R})$ with Lipschitz constant $\mathcal{L} > 0$. Then:*

i) $\left| \int_a^b [\mathcal{H}(Tf)\ (\mathcal{J}_F^\varphi)' - \mathcal{H}(Tg)\ (\mathcal{J}_G^\varphi)']dx \right| \le \mathcal{L}\|\varphi'\|_\infty \|f - g\|_1 \quad \forall f, g \in L^1(a,b),\ \forall \varphi \in C_c^\infty(\mathcal{I});$

ii) $\exists C > 0,\ \left| \int_a^b [\mathcal{H}(Tf)\ (\mathcal{G}^{F,\psi})' - \mathcal{H}(Tg)\ (\mathcal{G}^{G,\psi})']dx \right| \le C\|F - G\|_{W^{1,1}} \quad \forall f, g \in L^1(a,b),\ \forall \psi \in C_c^\infty(\mathcal{I}).$

We conclude this section with a statement on the continuous dependence of $(\mathcal{J}^\varphi)'$ with respect to f.

Proposition 2.15. *Let $f, f_n \in C^1(\bar{\mathcal{I}})$, $n \in \mathbb{N}$, satisfy assumption* (2.9)*, assume that the sequence $\{f_n\}$ converges uniformly to f, and let $\varphi \in C_c^\infty(\mathcal{I})$. Denote by $\mathcal{J}^\varphi$ the function related to f defined in* (2.10) *and by $\mathcal{J}_n^\varphi$ the corresponding function related to f_n. Then*

$$\|\mathcal{J}_n^\varphi - \mathcal{J}^\varphi\|_1 \to 0, \qquad \|(\mathcal{J}_n^\varphi)' - (\mathcal{J}^\varphi)'\|_1 \to 0.$$

3 Energy balance in a suspension bridge

3.1 The energy of the deck

In this section we define all the energetic contributions involved in the cable-hangers-beam system aiming to derive the variational form of the problem. In Figure 6 is sketched a cross section of the bridge, in which the degrees of freedom $w(x,t)$ and $\theta(x,t)$ correspond respectively to the downward displacement and the torsional angle around the barycentric line of the deck.

We do not consider the masses of the hangers and of the cables, since they are negligible with respect to the mass of the deck. The deformations of the deck deriving from bending and torsion are modeled, as for a beam, according to the de Saint Venant and Vlasov theory: the deck is characterized by the flexural rigidity EI, the torsional rigidity GK (by de Saint Venant) and the torsional warping EJ (by Vlasov [29]). The energy of the deck is given by the kinetic, the gravitational and the deformation contributions. The first depends on the vertical displacement and the rotation of the deck, i.e.

$$E_k = \frac{M}{2} \int_0^L w_t^2\, dx + \frac{M\ell^2}{6} \int_0^L \theta_t^2\, dx,$$

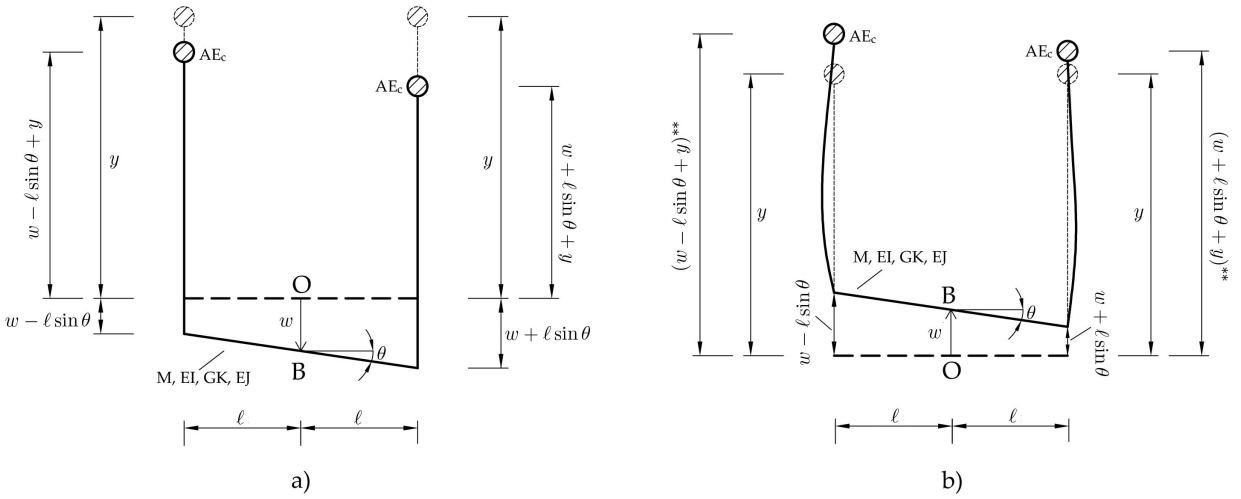

Figure 6: Mutual positions of the cross section of the bridge and of the cables.

where M is the mass linear density of the deck and ℓ is the semi width of the deck. The gravitational energy is due to dead loads and is negative because w is positive downwards,

$$E_g = -Mg \int_0^L w \, dx.$$

The deformation energy is given by the bending energy and the torsional energy

$$E_d = \frac{EI}{2} \int_0^L w_{xx}^2 \, dx + \frac{GK}{2} \int_0^L \theta_x^2 \, dx + \frac{EJ}{2} \int_0^L \theta_{xx}^2 \, dx.$$

Here, E is the Young modulus, G is the shear modulus, I is the moment of inertia, K is the torsional constant and J is the warping constant of the cross section. The last term was added by Vlasov [29] to the de Saint Venant's deformation terms.

3.2 The deformation energy of the cables

We assume that the cables have the same mechanical properties and, at rest, they take a parabolic shape $y(x)$ given by

$$y(x) = -\frac{Mg}{4H} x^2 + \frac{MgL}{4H} x - y_0 \qquad \forall x \in [0, L]\,, \tag{3.1}$$

in which H is the tension of the cable, Mg is the weight of the deck, L is the length of the bridge span and y_0 is the height of the towers, see again Figure 1. For details on the derivation of (3.1) we refer to [22]. Thanks to the equilibrium we have $H = \frac{MgL^2}{16f}$, where f is the cable sag as in Figure 1. Hence, (3.1) can be written as

$$y(x) = -\frac{4f}{L^2} x^2 + \frac{4f}{L} x - y_0 \qquad \forall x \in [0, L],$$

and the local length of the cables is given for all $x \in [0, L]$ by the bounded function

$$\xi(x) := \sqrt{1 + y'(x)^2}, \qquad 1 \le \xi(x) \le \xi_M := \sqrt{1 + \left(\frac{4f}{L}\right)^2}.$$

From [25, p.68] we know that in bridge design the sag-span ratio f/L varies between 1/12 and 1/8, implying a little variation of $\xi(x)$ on $[0, L]$; indeed, its maximum value, assumed for $x \in \{0, L\}$, is

$$\xi(0) = \xi(L) = \xi_M \in \left[\frac{\sqrt{10}}{3}, \frac{\sqrt{5}}{2}\right] = [1.05, 1.11].$$

In engineering literature $\xi(x)$ is often approximated with 1, see [22]. But $\xi(x)$ remains closer to its mean value $\overline{\xi}$ over the interval $[0, L]$; for these reasons we shall use the approximation

$$\xi(x) \approx \overline{\xi} := \frac{\int_0^L \xi(x)dx}{L}. \tag{3.2}$$

We point out that for the TNB, $\xi_M = 1.05$ and $\overline{\xi} = 1.02$ so that, by assuming (3.2), the maximum error is less than 2.86%. We refer to Section 4.3 for some issues related to the presence of the non approximated $\xi(x)$ in our system and to the consequences that this function produces on the system in terms of existence and uniqueness of a solution.

To obtain the energy of the cables we need to find their convexified shapes. Let us clarify how we apply the procedure explained in Section 2.1. In Figure 6a) is shown the situation with tensioned hangers, in which the edges of the deck have moved downwards of $w \pm \ell \sin\theta$. In this case, the cables maintain their convex shape and the hangers behave like inextensible elements so that the cables have the same displacement of the deck and their positions are equal to $(w \pm \ell \sin\theta + y)$. In Figure 6b) we represent the innovative part of our model. If the endpoints of the cross section of the deck move upwards, above the position $(w \pm \ell \sin\theta + y) = 0$, then the slackening of the hangers may occur, producing a vertical displacement in the cables equal to $(w \pm \ell \sin\theta + y)^{**}$. The shape of the cables is then given by the convexification of the function $(w \pm \ell \sin\theta + y)$, that depends not only on x, but also on t. To determine the deformation energy of a cable we need to compute its variation of length with respect to its initial length L_c. To this end, we introduce the functional $\Gamma : C^1[0, L] \to \mathbb{R}$ defined by

$$\Gamma(u) := \int_0^L \big(\sqrt{1 + \{[(u + y)^{**}]_x\}^2} - \sqrt{1 + (y')^2}\big)dx = \int_0^L \big(\sqrt{1 + \{[(u + y)^{**}]_x\}^2}\big)dx - L_c. \tag{3.3}$$

$\Gamma(u)$ is well-defined, since the convexification preserves the C^1-regularity of u. The deformation energy E_C of the cables is composed by two contributions. The first is related to the tension at rest and the second to the additional tension due to the increment of the length $\Gamma(w \pm \ell \sin\theta)$ of each cable. Hence if $\overline{\xi}$ is as in (3.2), we have

$$\begin{aligned} E_C =& H\overline{\xi} \int_0^L \left(\sqrt{1 + \{[(w + \ell \sin\theta + y)^{**}]_x\}^2} + \sqrt{1 + \{[(w - \ell \sin\theta + y)^{**}]_x\}^2} - 2\sqrt{1 + (y')^2}\right) dx \\ &+ \frac{AE_c}{2L_c}\big([\Gamma(w + \ell \sin\theta)]^2 + [\Gamma(w - \ell \sin\theta)]^2\big), \end{aligned} \tag{3.4}$$

in which H is the horizontal tension, A the sectional area and E_c the Young modulus of the cable.

3.3 Functional spaces and total energy of the system

We consider the Hilbert spaces $L^2(0, L)$, $H_0^1(0, L)$ and $H^2 \cap H_0^1(0, L)$, endowed respectively with the scalar products

$$(u, v)_2 = \int_0^L uv, \quad (u, v)_{H^1} = \int_0^L u'v', \quad (u, v)_{H^2} = \int_0^L u''v''.$$

We denote by $H^*(0, L)$ the dual space of $H^2 \cap H_0^1(0, L)$ with the corresponding duality denoted by $\langle \cdot, \cdot \rangle_*$. The solutions of the equations are required to satisfy $(w, \theta) \in X_T^2$, where

$$X_T := C^0\big([0, T]; H^2 \cap H_0^1(0, L)\big) \cap C^1\big([0, T]; L^2(0, L)\big) \cap C^2\big([0, T]; H^*(0, L)\big). \tag{3.5}$$

Then, by adding all the energetic contributions of the system, for every $(w,\theta) \in X_T^2$ we find the functional

$$\begin{aligned}\mathcal{E}(w,\theta) := &\int_0^L \left(\frac{M}{2}w_t^2 + \frac{M\ell^2}{6}\theta_t^2\right) dx + \int_0^L \left(\frac{EI}{2}w_{xx}^2 + \frac{EJ}{2}\theta_{xx}^2 + \frac{GK}{2}\theta_x^2\right)dx - Mg\int_0^L w\,dx \\ &+ H\overline{\xi}\Big\{\int_0^L \big(\sqrt{1+\{[(w+\ell\sin\theta+y)^{**}]_x\}^2} + \sqrt{1+\{[(w-\ell\sin\theta+y)^{**}]_x\}^2}\big)dx - 2L_c\Big\} \\ &+ \frac{AE_c}{2L_c}\big([\Gamma(w+\ell\sin\theta)]^2 + [\Gamma(w-\ell\sin\theta)]^2\big),\end{aligned} \tag{3.6}$$

that is well-defined and represents the energy of the system.

Proposition 3.1. *The functional $\mathcal{E} : X_T^2 \to \mathbb{R}$ is locally Lipschitz continuous.*

Proof. The Proposition holds if, for every bounded subset $X \subset X_T^2$ there exists $\mathcal{L} > 0$ such that, given (w_1,θ_1) and $(w_2,\theta_2) \in X$ we have

$$|\mathcal{E}(w_1,\theta_1) - \mathcal{E}(w_2,\theta_2)| \le \mathcal{L}\big(||(w_1-w_2)_t||_1 + ||(\theta_1-\theta_2)_t||_1 + ||w_1-w_2||_{W^{2,1}} + ||\theta_1-\theta_2||_{W^{2,1}}\big). \tag{3.7}$$

By (3.6) we observe that the most tricky terms are those including $\Gamma(\cdot)$ and $\overline{\xi}$, while for the others (3.7) is easily proved. Let us recall the inequality

$$|\sqrt{1+(u_1+v)^2} - \sqrt{1+(u_2+v)^2}| \le |(u_1+v)-(u_2+v)| = |u_1-u_2| \quad \forall u_1,u_2,v \in \mathbb{R},$$

that gives

$$\begin{aligned}&\big|\sqrt{1+\{[(w_1 \pm \ell\sin\theta_1+y)^{**}]_x\}^2} - \sqrt{1+\{[(w_2 \pm \ell\sin\theta_2+y)^{**}]_x\}^2}\big| \\ &\le \big|[(w_1 \pm \ell\sin\theta_1+y)^{**} - (w_2 \pm \ell\sin\theta_2+y)^{**}]_x\big|.\end{aligned}$$

Hence, it is possible to apply Proposition 2.11 so that there exists $L_1 > 0$ such that

$$\begin{aligned}&H\overline{\xi}\int_0^L \big|\sqrt{1+\{[(w_1 \pm \ell\sin\theta_1+y)^{**}]_x\}^2} - \sqrt{1+\{[(w_2 \pm \ell\sin\theta_2+y)^{**}]_x\}^2}\big|dx \\ &\le H\overline{\xi}\big(||(w_1-w_2)_x||_1 + \ell||(\sin\theta_1-\sin\theta_2)_x||_1\big) \le L_1\big(||(w_1-w_2)_x||_1 + ||\theta_1-\theta_2||_{W^{1,1}}\big).\end{aligned}$$

The same argument can be applied to the terms $[\Gamma(w \pm \ell\sin\theta)]^2$, see (3.3). □

This result enables us to use the notion of Clarke subdifferential [13] and to compute the variation of (3.6) in the general framework of the differential inclusions.

4 Suspension bridges with convexified cables

4.1 The variation of the deformation energy of the cables

The presence of the convexified functions within the functional $\mathcal{E}(w,\theta)$ in (3.6) introduces some difficulties in computing its variation; from Proposition 2.2 the unilateral Gateaux derivative exists and is always bounded, while the Gateaux derivative may not exist in some special cases.

Let us focus on one cable, the other being similar. We introduce

$$D^- := \big[H\overline{\xi} + \frac{AE_c}{L_c}\Gamma(w+\ell\sin\theta)\big]\int_0^L \frac{[(w+\ell\sin\theta+y)^{**}]_x(\mathcal{J}_-^{\varphi})'}{\sqrt{1+\{[(w+\ell\sin\theta+y)^{**}]_x\}^2}}\,dx$$

$$D^+ := \big[H\overline{\xi} + \frac{AE_c}{L_c}\Gamma(w+\ell\sin\theta)\big]\int_0^L \frac{[(w+\ell\sin\theta+y)^{**}]_x(\mathcal{J}_+^\varphi)'}{\sqrt{1+\{[(w+\ell\sin\theta+y)^{**}]_x\}^2}}\,dx,$$

where $\mathcal{J}_\pm^\varphi(x)$ are defined in (2.8) with $f = (w+\ell\sin\theta+y)$. By applying Proposition 2.2, we find the following inclusion related to the variation of the energy (3.4) with respect to w

$$\langle dE_C(w,\theta),\varphi\rangle \in \big[\min\{D^-,D^+\},\max\{D^-,D^+\}\big].$$

To avoid this heavy notation, in the sequel we always write

$$\langle dE_C(w,\theta),\varphi\rangle \in \big[H\overline{\xi} + \frac{AE_c}{L_c}\Gamma(w+\ell\sin\theta)\big]\int_0^L \frac{[(w+\ell\sin\theta+y)^{**}]_x(\mathcal{J}_\pm^\varphi)'}{\sqrt{1+\{[(w+\ell\sin\theta+y)^{**}]_x\}^2}}\,dx \quad \forall\varphi\in C_c^\infty(\mathcal{I}).$$

By applying Theorem 2.8 with $\Lambda(\theta) = \sin\theta$ we obtain the inclusion related to the variation of the energy (3.4) with respect to θ

$$\langle dE_C(w,\theta),\psi\rangle \in \big[H\overline{\xi} + \frac{AE_c}{L_c}\Gamma(w+\ell\sin\theta)\big]\ell\int_0^L \frac{[(w+\ell\sin\theta+y)^{**}]_x(\mathcal{G}_\pm^{\theta,\psi})_x}{\sqrt{1+\{[(w+\ell\sin\theta+y)^{**}]_x\}^2}}\,dx \quad \forall\psi\in C_c^\infty(\mathcal{I}),$$

where $\mathcal{G}_\pm^{\theta,\psi}(x)$ is defined for every $t\geq 0$ fixed, in analogy with $\mathcal{J}_\pm^\varphi(x)$ as

$$\mathcal{G}_\pm^{\theta,\psi}(x) := \begin{cases} \pm(\pm g_i^\pm)^{**}(x) & x\in K^i,\ i\in J_C,\\ \psi(x)\cos\big(\theta(x)\big) & x\in\widetilde{K}_f, \end{cases} \tag{4.1}$$

with

$$g_i^\pm\colon K^i\to\overline{\mathbb{R}}, \qquad g_i^\pm(x) := \begin{cases} \psi(x)\cos\big(\theta(x)\big) & x\in K^i\cap(K_f\cup\{a,b\}),\\ \pm\infty & x\in K^i\setminus(K_f\cup\{a,b\}). \end{cases}$$

Note that the functions $\mathcal{J}_\pm^\varphi$ and $\mathcal{G}_\pm^{\theta,\psi}$ are spatially continuous with a finite number of angular points, so that $(\mathcal{J}_\pm^\varphi)'$ and $(\mathcal{G}_\pm^{\theta,\psi})_x$ are bounded on the interval $[0,L]$ and continuous almost everywhere in $[0,L]$, see Remark 2.5.

In the simple cases in which the cable is strictly convex (or concave!) we gain the differentiability of (3.6) and the inclusions become equalities. In the first case, because $\widetilde{K}_f = \mathcal{I}$ so that $\mathcal{J}_\pm^\varphi$ and $\mathcal{G}_\pm^{\theta,\psi}$ coincide respectively with φ and $\psi\cos\theta$. In the second case, $K^1 = \overline{I}^1 = \overline{\mathcal{I}}$ so that $\mathcal{I}^\varphi = \mathcal{G}^{\theta,\psi} = 0$ and $(w+\ell\sin\theta+y)^{**} = -y_0$ for all $x\in[0,L]$; this situation corresponds to a zero variation in the cable energy since the slackening of all the hangers occurs, implying the total disconnection between the cable and the deck. We point out that in the case where the cable is perfectly horizontal we obtain the same physical result, due to $(w+\ell\sin\theta+y)_x = [(w+\ell\sin\theta+y)^{**}]_x = 0$ for all $x\in[0,L]$, while $\mathcal{I}_\pm^\varphi$ and $\mathcal{G}_\pm^{\theta,\psi}$ maintain their oscillatory nature.

4.2 The system of partial differential inclusions

In this section we state the problem in the general framework of partial differential inclusions, resulting from the variation of (3.6). To this aim we introduce the subscripts α and β to denote the terms corresponding respectively to the cable with shape $(w+\ell\sin\theta+y)^{**}$ and $(w-\ell\sin\theta+y)^{**}$; in this way we have $\mathcal{J}_{\alpha\pm}^\varphi(x)$, $\mathcal{G}_{\alpha\pm}^{\theta,\psi}(x)$ and $\mathcal{J}_{\beta\pm}^\varphi(x)$, $\mathcal{G}_{\beta\pm}^{\theta,\psi}(x)$ that correspond to $\mathcal{J}_\pm^\varphi(x)$, $\mathcal{G}_\pm^{\theta,\psi}(x)$ related respectively to $f_\alpha = (w+\ell\sin\theta+y)$ and $f_\beta = (w-\ell\sin\theta+y)$, as defined in (2.8) and (4.1).

As for the action, one has to take the difference between kinetic energy and potential energy and integrate over an interval of time $[0,T]$:

$$\begin{aligned}\mathcal{A}(w,\theta) := \int_0^T \Bigg[\int_0^L \left(\frac{M}{2}w_t^2 + \frac{M\ell^2}{6}\theta_t^2\right) dx - \int_0^L \left(\frac{EI}{2}w_{xx}^2 + \frac{EJ}{2}\theta_{xx}^2 + \frac{GK}{2}\theta_x^2\right)dx + Mg\int_0^L w\,dx \\ - H\bar{\xi}\Bigg\{ \int_0^L \big(\sqrt{1+\{[(w+\ell\sin\theta+y)^{**}]_x\}^2} + \sqrt{1+\{[(w-\ell\sin\theta+y)^{**}]_x\}^2}\big)dx - 2L_c\Bigg\} \\ - \frac{AE_c}{2L_c}\big([\Gamma(w+\ell\sin\theta)]^2 + [\Gamma(w-\ell\sin\theta)]^2\big)\Bigg] dt.\end{aligned}$$

The differential inclusion describing the motion of the bridge is obtained by considering the critical points of the functional $\mathcal{A}$, which leads to the following

Definition 4.1. *We say that $(w,\theta) \in X_T^2$, see (3.5), is a weak solution of the differential inclusion, resulting from critical points of the action $\mathcal{A}$, if (w,θ) satisfies*

$$\begin{cases} M\langle w_{tt},\varphi\rangle_* + EI(w,\varphi)_{H^2} - \big(Mg,\varphi\big)_2 \in \\ \qquad -\big[H\bar{\xi} + \frac{AE_c}{L_c}\Gamma(w+\ell\sin\theta)\big]\left(\dfrac{[(w+\ell\sin\theta+y)^{**}]_x}{\sqrt{1+\{[(w+\ell\sin\theta+y)^{**}]_x\}^2}}, (\mathcal{J}_{\alpha\pm}^{\varphi})'\right)_2 \\ \qquad -\big[H\bar{\xi} + \frac{AE_c}{L_c}\Gamma(w-\ell\sin\theta)\big]\left(\dfrac{[(w-\ell\sin\theta+y)^{**}]_x}{\sqrt{1+\{[(w-\ell\sin\theta+y)^{**}]_x\}^2}}, (\mathcal{J}_{\beta\pm}^{\varphi})'\right)_2, \\ \dfrac{M\ell}{3}\langle\theta_{tt},\psi\rangle_* + \dfrac{EJ}{\ell}(\theta,\psi)_{H^2} + \dfrac{GK}{\ell}(\theta,\psi)_{H^1} \in \\ \qquad -\big[H\bar{\xi} + \frac{AE_c}{L_c}\Gamma(w+\ell\sin\theta)\big]\left(\dfrac{[(w+\ell\sin\theta+y)^{**}]_x}{\sqrt{1+\{[(w+\ell\sin\theta+y)^{**}]_x\}^2}}, (\mathcal{G}_{\alpha\pm}^{\theta,\psi})_x\right)_2 \\ \qquad +\big[H\bar{\xi} + \frac{AE_c}{L_c}\Gamma(w-\ell\sin\theta)\big]\left(\dfrac{[(w-\ell\sin\theta+y)^{**}]_x}{\sqrt{1+\{[(w-\ell\sin\theta+y)^{**}]_x\}^2}}, (\mathcal{G}_{\beta\pm}^{\theta,\psi})_x\right)_2, \end{cases} \tag{4.2}$$

for all $\varphi,\psi \in H^2 \cap H_0^1(0,L)$ and $t>0$.

The system (4.2) is complemented with the initial conditions:

$$\begin{aligned} &w(x,0) = w^0(x), \quad \theta(x,0) = \theta^0(x) && \text{for } x \in (0,L) \\ &w_t(x,0) = w^1(x), \quad \theta_t(x,0) = \theta^1(x) && \text{for } x \in (0,L), \end{aligned} \tag{4.3}$$

having the following regularity

$$w^0,\theta^0 \in H^2 \cap H_0^1(0,L), \qquad w^1,\theta^1 \in L^2(0,L). \tag{4.4}$$

From [5, 12, 13] we learn that to prove existence results for a differential inclusion can be a difficult task, requiring some regularity assumptions on the right hand side terms, e.g. the continuity. For our purposes to approach problem (4.2)-(4.3) in fully generality is not really necessary: since we are dealing with the modeling of a civil structure, it is possible to perform some simplifications. We follow a suggestion from [7, p.23] which says that

> ... out of the infinite number of possible modes of motion in which a suspension bridge might vibrate, we are interested only in a few, to wit: the ones having the smaller numbers of loops or half waves.

Indeed, civil structures typically oscillate on low modes since higher modes do not appear in realistic situations due to very large bending energy, see [7, 28]. This suggestion mathematically corresponds to project an infinite dimensional space on a finite dimensional subspace, using the Galerkin approximation.

To this aim, we take $\{e_k\}_{k=1}^{\infty}$ as an orthogonal basis of $L^2(0,L)$, $H_0^1(0,L)$, $H^2\cap H_0^1(0,L)$, where

$$e_k(x)=\sqrt{\frac{2}{L}}\sin\left(\frac{k\pi x}{L}\right),\qquad ||e_k||_2=1,\qquad ||e_k||_{H^1}=\frac{k\pi}{L},\qquad ||e_k||_{H^2}=\frac{k^2\pi^2}{L^2},$$

and, for any $n\geq 1$, we introduce the space $E_n:=\mathrm{span}\{e_1,\dots,e_n\}$. For any $n\geq 1$ we seek a couple $(w_n,\theta_n)\in X_T^2$ such that

$$w_n(x,t)=\sum_{k=1}^{n}w_n^k(t)\,e_k(x),\qquad \theta_n(x,t)=\sum_{k=1}^{n}\theta_n^k(t)\,e_k(x),$$

and satisfying (4.2) only for the test functions $\varphi,\psi\in E_n$, thereby obtaining a finite system of ordinary differential inclusions. In fact, in this finite dimensional setting, the inclusions become equalities, since for every fixed $n\in\mathbb{N}$, all the intervals of affinity (if any) of $(w_n\pm\ell\sin\theta_n+y)^{**}$ are such that

$$(w_n\pm\ell\sin\theta_n+y)>(w_n\pm\ell\sin\theta_n+y)^{**}.$$

Then Corollary 2.3 applies and the Gateaux derivative exists, leading to a finite system of ordinary differential equations

$$\begin{cases} M\big((w_n)_{tt},e_r\big)_2+EI\big(w_n,e_r\big)_{H^2}-(Mg,e_r)_2= \\ \qquad -\big[H\overline{\xi}+\frac{AE_c}{L_c}\Gamma(w_n+\ell\sin\theta_n)\big]\left(\dfrac{[(w_n+\ell\sin\theta_n+y)^{**}]_x}{\sqrt{1+\{[(w_n+\ell\sin\theta_n+y)^{**}]_x\}^2}},[\mathfrak{I}_\alpha^{e_r}]'\right)_2 \\ \qquad -\big[H\overline{\xi}+\frac{AE_c}{L_c}\Gamma(w_n-\ell\sin\theta_n)\big]\left(\dfrac{[(w_n-\ell\sin\theta_n+y)^{**}]_x}{\sqrt{1+\{[(w_n-\ell\sin\theta_n+y)^{**}]_x\}^2}},[\mathfrak{I}_\beta^{e_r}]'\right)_2 \\ \dfrac{M\ell}{3}\big((\theta_n)_{tt},e_r\big)_2+\dfrac{EJ}{\ell}\big(\theta_n,e_r\big)_{H^2}+\dfrac{GK}{\ell}\big(\theta_n,e_r\big)_{H^1}= \\ \qquad -\big[H\overline{\xi}+\frac{AE_c}{L_c}\Gamma(w_n+\ell\sin\theta_n)\big]\left(\dfrac{[(w_n+\ell\sin\theta_n+y)^{**}]_x}{\sqrt{1+\{[(w_n+\ell\sin\theta_n+y)^{**}]_x\}^2}},[\mathfrak{I}_\alpha^{\theta_n,e_r}]_x\right)_2 \\ \qquad +\big[H\overline{\xi}+\frac{AE_c}{L_c}\Gamma(w_n-\ell\sin\theta_n)\big]\left(\dfrac{[(w_n-\ell\sin\theta_n+y)^{**}]_x}{\sqrt{1+\{[(w_n-\ell\sin\theta_n+y)^{**}]_x\}^2}},[\mathfrak{I}_\beta^{\theta_n,e_r}]_x\right)_2, \end{cases} \tag{4.5}$$

for $r=1,\dots,n$, with the initial conditions

$$w_n^k(0)=(w^0,e_k)_2,\qquad \theta_n^k(0)=(\theta^0,e_k)_2\qquad \dot{w}_n^k(0)=(w^1,e_k)_2,\qquad \dot{\theta}_n^k(0)=(\theta^1,e_k)_2. \tag{4.6}$$

In Section 7 we prove

Theorem 4.2. *Let $n\geq 1$ an integer and $T>0$ (including the case $T=\infty$), then for all $w^0,\theta^0,w^1,\theta^1$ satisfying (4.4) there exists a unique solution $(w_n,\theta_n)\in X_T^2$ of (4.5) which satisfies (4.6).*

This justifies the following

Definition 4.3. *For all $n\in\mathbb{N}$, we say that the solution (w_n,θ_n) of (4.5)-(4.6) is an **approximate solution** of (4.2)-(4.3).*

Among the solutions of (4.2)-(4.3) we are interested in those being approximable, according to

Definition 4.4. *We say that $(w,\theta)\in X_T^2$ is an **approximable solution** of (4.2)-(4.3) if there exists a sequence of approximate solutions of (4.2)-(4.3), converging to it as $n\to\infty$, up to a subsequence.*

We state now the main result of this section.

Theorem 4.5. *Let $T>0$ (including the case $T=\infty$), then for all $w^0,\theta^0,w^1,\theta^1$ satisfying (4.4) there exists an approximable solution of (4.2) which satisfies (4.3) on $[0,T]$.*

The proof of Theorem 4.5 is given in Section 7.

Remark 4.6. The results obtained in this section on the approximate solution (w_n,θ_n) can be achieved in the same way considering a different number of modes for w and θ, i.e. taking (w_n,θ_ν) with $n\neq\nu$.

4.3 A remark on the approximation (3.2)

Let us write (4.5) more simply, including all the nonlinearities of the system into the functionals

$$h_\alpha(w_n,\theta_n) := -\left(H\overline{\xi}+\frac{AE_c}{L_c}\Gamma(w_n+\ell\sin\theta_n)\right)\frac{[(w_n+\ell\sin\theta_n+y)^{**}]_x}{\sqrt{1+\{[(w_n+\ell\sin\theta_n+y)^{**}]_x\}^2}}$$
$$h_\beta(w_n,\theta_n) := -\left(H\overline{\xi}+\frac{AE_c}{L_c}\Gamma(w_n-\ell\sin\theta_n)\right)\frac{[(w_n-\ell\sin\theta_n+y)^{**}]_x}{\sqrt{1+\{[(w_n-\ell\sin\theta_n+y)^{**}]_x\}^2}}.$$

Testing n times the equations (4.5) for $r=1,\dots,n$ and $t\geq 0$ we obtain a system of ordinary differential equations for all $k=1,\dots,n$

$$\begin{cases} M\ddot{w}_n^k(t)+EI\dfrac{k^4\pi^4}{L^4}w_n^k(t)+Mg\dfrac{\sqrt{2L}((-1)^k-1)}{k\pi} = \big(h_\alpha(w_n,\theta_n),[\mathcal{J}_\alpha^{e_k}]'\big)_2+\big(h_\beta(w_n,\theta_n),[\mathcal{J}_\beta^{e_k}]'\big)_2 \\ \dfrac{M\ell}{3}\ddot{\theta}_n^k(t)+\left(EJ\dfrac{k^4\pi^4}{L^4\ell}+GK\dfrac{k^2\pi^2}{L^2\ell}\right)\theta_n^k(t) = \big(h_\alpha(w_n,\theta_n),[\mathcal{G}_\alpha^{\theta_n,e_k}]_x\big)_2-\big(h_\beta(w_n,\theta_n),[\mathcal{G}_\beta^{\theta_n,e_k}]_x\big)_2 \end{cases} \tag{4.7}$$

with the initial conditions (4.6).

In Section 3.2 we have approximated the function $\xi(x)$ with its mean value $\overline{\xi}$ assumed on $[0,L]$. In this section we present some observations related to system (4.7) without assuming (3.2). Even if $\xi(x)$ does not depend on the solution and is a smooth and bounded function on $[0,L]$, its presence generates some problems related to the existence and uniqueness of (w_n^k,θ_n^k).

In this case it is possible to apply for the existence result a fixed point argument; in particular, we introduce the vectors $Z(t)=[z_n^1(t),\dots,z_n^n(t)]\in C^1(\mathbb{R})$, $\Pi(t)=[\Pi_n^1(t),\dots,\Pi_n^n(t)]\in C^1(\mathbb{R})$ and $e(x)=[e_1(x),\dots,e_n(x)]\in C^\infty([0,L])$ and we plug them into the right hand side terms of (4.7). Hence, we obtain

$$F_k(t) := \int_0^L\left[H\xi(x)+\frac{AE_c}{L_c}\Gamma\big(Z\cdot e+\ell\sin(\Pi\cdot e)\big)\right]\chi\left([Z\cdot e+\ell\sin(\Pi\cdot e)+y]^{**}\right)(\mathcal{J}_\alpha^{e_k})'dx;$$

note that Proposition 2.14 does not hold, since the fundamental identity (6.14) (see Section 6) is not verified and the locally Lipschitz continuity is not assured (similarly for $G_k(t)$). Proposition 2.15 guarantees that $F_k(t)$ and $G_k(t)$ are time continuous for all $k=1,\dots,n$, indeed, taking $t_j\to t$, and following the scheme of the proof of Theorem 4.2, we have $K>0$ such that

$$|F_k(t_j)-F_k(t)|\leq K(\|Z(t_j)\cdot e-Z(t)\cdot e\|_1+\|\Pi(t_j)\cdot e-\Pi(t)\cdot e\|_{W^{1,1}}+\|(\mathcal{J}_\alpha^{e_k}(t_j)-\mathcal{J}_\alpha^{e_k}(t))'\|_1)\to 0,$$

for all $k=1,\dots,n$.

Thanks to the classical ordinary differential equation (ODE) theory there exists a solution $(\Phi w_n^k(t),\Psi\theta_n^k(t))\in C^2[0,t_n)\times C^2[0,t_n)$ for all $k=1,\dots,n$ and for $t_n\in(0,T]$ of the linear problem

$$\begin{cases} M\ddot{\Phi}w_n^k(t)+EI\dfrac{k^4\pi^4}{L^4}\Phi w_n^k(t)+Mg\dfrac{\sqrt{2L}((-1)^k-1)}{k\pi} = \big(h_\alpha(Z\cdot e,\Pi\cdot e),[\mathcal{J}_\alpha^{e_k}]'\big)_2+\big(h_\beta(Z\cdot e,\Pi\cdot e),[\mathcal{J}_\beta^{e_k}]'\big)_2 \\ \dfrac{M\ell}{3}\ddot{\Psi}\theta_n^k(t)+\left(EJ\dfrac{k^4\pi^4}{L^4\ell}+GK\dfrac{k^2\pi^2}{L^2\ell}\right)\Psi\theta_n^k(t) = \big(h_\alpha(Z\cdot e,\Pi\cdot e),[\mathcal{G}_\alpha^{\Pi\cdot e,e_k}]_x\big)_2-\big(h_\beta(Z\cdot e,\Pi\cdot e),[\mathcal{G}_\beta^{\Pi\cdot e,e_k}]_x\big)_2 \end{cases}$$

with the initial conditions

$$\Phi w_n^k(0)=(w^0,e_k)_2,\qquad \Psi\theta_n^k(0)=(\theta^0,e_k)_2\qquad \dot{\Phi}w_n^k(0)=(w^1,e_k)_2,\qquad \dot{\Psi}\theta_n^k(0)=(\theta^1,e_k)_2.$$

Now we choose $\Phi w_n^k(t)$ and $\Psi\theta_n^k(t)$ as the components of the vectors $Z(t)$ and $\Pi(t)$ and we plug them into (4.7). In this way we obtain two operators $\Phi: C^1([0,t_n))\to C^1([0,t_n))$, $\Psi: C^1([0,t_n))\to C^1([0,t_n))$ that are compact due to the compact embedding $C^2\subset C^1$, so that there exists a fixed point $\Phi w_n^k=w_n^k$ and $\Psi\theta_n^k=\theta_n^k$ for all $k=1,\dots,n$, thanks to the Schauder fixed point theorem; this implies the existence of a solution on some $[0,t_n)$ for $t_n\in(0,T]$, while the global existence on $[0,T]$ can be deduced as in the proof of Theorem 4.2.

5 Numerical results

In this section we present some numerical experiments on the system (4.5)-(4.6). The results are obtained with the software Matlab®, adopting the mechanical constants of the TNB in Table 1.

E:	210 000MPa	Young modulus of the deck (steel)
E_c:	185 000MPa	Young modulus of the cables (steel)
G:	81 000MPa	Shear modulus of the deck (steel)
L:	853.44m	Length of the main span
ℓ :	6m	Half width of the deck
f:	70.71m	Sag of the cable
I:	0.154m^4	Moment of inertia of the deck cross section
K:	$6.07{\cdot}10^{-6}\text{m}^4$	Torsional constant of the deck
J:	5.44m^6	Warping constant of the deck
A:	0.1228m^2	Area of the cables section
M:	7198kg/m	Mass linear density of the deck
H:	45 413kN	Initial tension in the cables
L_c:	868.815m	Initial length of the cables, see (3.3)

Table 1: TNB mechanical constants.

When we speak about a mode like $\sin\left(\frac{k\pi}{L}x\right)$, we refer to a motion with $k-1$ nodes, in which the latter are the zeros of the sine function in $(0, L)$. Let recall some meaningful witnesses that led our modeling choices. From [1, p.28] we know that for the TNB

> seven different motions have been definitely identified on the main span of the bridge.

The most common appears to be the 2 nodes mode, like $\sin\left(\frac{3\pi}{L}x\right)$. The morning of the failure Farquharson, a witness of the collapse described a torsional motion like $\sin\left(\frac{2\pi}{L}x\right)$, writing [1, V-2]

> a violent change in the motion was noted. [...] the motions, which a moment before had involved a number of waves (nine or ten) had shifted almost instantly to two [...] the node was at the center of the main span and the structure was subjected to a violent torsional action about this point.

Thanks to Theorem 4.5 we may consider an approximable solution of (4.2) and we must decide how many modes to include in the final dimensional approximation. From the Federal Report [1] we learn that, at the TNB, oscillations with more than 10 nodes on the main span were never seen. In our numerical experiments we consider the first 10 longitudinal modes interacting with the first 4 torsional modes; this is a good compromise between limiting computational burden and focusing on the instability phenomena visible at TNB. Moreover, we performed the same numerical experiments with a larger number of given modes and we did not find significant changes in the instability thresholds.

Given the boundary conditions, we seek solutions of (4.5) in the form

$$w(x,t) = \sum_{k=1}^{10} w_k(t)\, e_k, \qquad \theta(x,t) = \sum_{k=1}^{4} \theta_k(t)\, e_k \tag{5.1}$$

where $e_k(x) = \sqrt{\frac{2}{L}} \sin\left(\frac{k\pi x}{L}\right)$ and $\sqrt{\frac{2}{L}}$ is a pure number with no unit of measure. In this way we obtain a system of 14 ODEs as (4.7) with the initial conditions

$$w_k(0) = w_k^0 = (w^0, e_k)_2, \qquad \dot{w}_k(0) = w_k^1 = (w^1, e_k)_2, \qquad \forall k = 1, \dots, 10$$
$$\theta_k(0) = \theta_k^0 = (\theta^0, e_k)_2, \qquad \dot{\theta}_k(0) = \theta_k^1 = (\theta^1, e_k)_2 \qquad \forall k = 1, \dots, 4.$$

Definition 5.1. *We call* $\overline{w}_k(t) := \sqrt{\frac{2}{L}} w_k(t)$ ***k-th longitudinal mode*** *and* $\overline{\theta}_k(t) := \sqrt{\frac{2}{L}} \theta_k(t)$ ***k-th torsional mode****.*

Following Definition 5.1, we put $\overline{w}_k^0 := \sqrt{\frac{2}{L}} w_k^0$, $\overline{w}_k^1 := \sqrt{\frac{2}{L}} w_k^1$ and similarly for the θ initial conditions. Since we study an isolated system we assume that on the bridge there is a balance between damping and wind on an interval $[0, T]$ for sufficiently small $T > 0$. More precisely, we consider a time lapse of $[0, 120s]$, that represents a small time interval compared to 70 minutes of violent oscillations recorded during the TNB collapse [1], enough to see the possible sudden transfer of energy between modes. We study the system during its steady motion, in which the oscillation of a j-th longitudinal mode prevails, while we perturb all the other modes with an initial condition 10^{-3} smaller, i.e. in dimensionless form

$$\overline{w}_k^0 = 10^{-3} \cdot \overline{w}_j^0 \quad \forall k \neq j, \qquad \overline{\theta}_k^0 = \overline{w}_k^1 = \overline{\theta}_k^1 = 10^{-3} \cdot \overline{w}_j^0 \quad \forall k.$$

Following this approach we say that the initial energy of our system corresponds to that of the longitudinal mode excited and represents, indirectly, the wind energy introduced on the bridge through the so-called vortex shedding [27].

Based on the procedure described in Section 2.1, we approximate convexifications numerically. The verification of the tangency condition (2.3) should take place continuously for all $x \in \mathcal{I}$, which is impossible from a numerical point of view. Hence, we evaluate (2.3) in a finite number of points, obtained by the discretization of $\mathcal{I} = (0, L)$ with a certain step Δx (in our case $\Delta x = L/2000$). Following this scheme we obtain an algorithm converging to (2.4) as $\Delta x \to 0$, thanks to the boundedness of $\mathcal{I}$. More precisely we solve (4.7) passing properly to a system of first order ODEs, so that we apply an implicit ODEs algorithm, e.g. Crank-Nicolson or Runge-Kutta; the numerical work-flow of each temporal iteration is organized as follows: we compute in the order the affinity intervals of convexification of the two cables, we compute the spatial integrals by discretizing $[0, L]$, see the right hand side terms of (4.7), and we use these values to run the ODEs algorithm.

According to the Report [1, p.20], in the months prior to the collapse, *one principal mode of oscillation prevailed and the modes of oscillation frequently changed.* Therefore, we follow [18] and we consider that the approximate solution (5.1) has an initially prevailing longitudinal mode, that is, there exists $j = 1, ..., 10$ such that $w_j(0)$ is much larger than all the other initial data (both longitudinal and torsional). Then the j-th longitudinal mode is torsionally stable if the all the torsional components $\theta_k(t)$ remain small for all t. In our analysis we aim to be more precise and we give a *quantitative* characterization of "smallness". We consider thresholds of instability following the approach in [18] and we say that the j-th longitudinal mode is **torsionally unstable** if at least one torsional mode grows about 1 order in amplitude in the time lapse $[0, 120s]$. From a numerical point of view we define the **threshold of instability** of the j-th longitudinal mode excited as

$$W_j^0 := \left\{ \inf \overline{w}_j^0 : \ \max_k \left\{ \max_{t \in [0,T]} |\overline{\theta}_k(t)| \right\} \geq 10^{-2} \cdot \overline{w}_j^0 \right\}; \tag{5.2}$$

this condition allows us to obtain thresholds W_j^0 accurate enough for our purposes.

As explained in Section 3.2, through the procedure of convexification, we are able to simulate the slackening of the hangers. To have an idea of the slackening quantity occurring in our numerical

experiments, we identify the two cables by the subscripts α and β as in Section 4.2, and we recall that, in the numerical discretization, $[0,T]$ is equally divided in m time step; hence, we compute for each time step Δt_h $(h = 1,\dots,m)$ a measure of the percentage of hangers slackened as the ratio between the measure of the union of the intervals of linearity for each cable and the length of the deck L, i.e.

$$\mathcal{M}_h^\alpha := \frac{1}{L}\left|\bigcup_{i\in J_\alpha} I_\alpha^i\right| \qquad \mathcal{M}_h^\beta := \frac{1}{L}\left|\bigcup_{j\in J_\beta} I_\beta^j\right| \qquad \forall h = 1,\dots,m.$$

Since the angle of rotation is small, the two cables behave quite similarly and, therefore, we define a mean value of the **measure of slackening** as

$$\mathcal{M} = \frac{1}{2m}\left[\sum_{h=1}^{m}\mathcal{M}_h^\alpha + \sum_{h=1}^{m}\mathcal{M}_h^\beta\right]. \tag{5.3}$$

Our purpose is to compare the instability thresholds of the model with convexification to those of the same model without convexification, see [17], i.e. we study how the slackening of the hangers affects the system. In Table 2 we have this comparison in terms of initial energy and amplitude threshold of instability of the j-th longitudinal mode excited, computed following (5.2). For each numerical experiment we verified the energy conservation, ascertaining a relative error, $|(\max\mathcal{E}(t) - \min\mathcal{E}(t))/\mathcal{E}(0)|$, on the integration time $[0, 120s]$, less than $4\cdot10^{-3}$.

	Convexification (Slackening)			**No convexification** (Rigid hangers)	
Mode	W_j^0[m]	$\mathcal{E}(0)$[J]	$\mathcal{M}$[%]	W_j^0[m]	$\mathcal{E}(0)$[J]
1	4.09	$7.96\cdot10^7$	1.92	4.09	$7.96\cdot10^7$
2	8.37	$8.74\cdot10^7$	2.94	8.22	$8.37\cdot10^7$
3	4.89	$8.58\cdot10^7$	2.40	4.82	$8.23\cdot10^7$
4	5.35	$1.63\cdot10^8$	41.79	4.92	$1.35\cdot10^8$
5	4.25	$1.77\cdot10^8$	39.40	3.93	$1.52\cdot10^8$
6	3.64	$1.64\cdot10^8$	43.46	2.64	$8.72\cdot10^7$
7	3.65	$2.38\cdot10^8$	51.72	5.25	$8.29\cdot10^8$
8	3.28	$2.27\cdot10^8$	50.05	5.15	$1.12\cdot10^9$
9	2.31	$1.54\cdot10^8$	42.55	3.87	$7.40\cdot10^8$
10	2.65	$2.34\cdot10^8$	52.73	3.41	$6.97\cdot10^8$

Table 2: Thresholds of instability as in (5.2), corresponding energy and measure of slackening as in (5.3), varying the longitudinal mode excited on $[0, 120s]$.

From the data in Table 2 we notice different tendencies depending on the mode excited. The first 3 longitudinal modes give substantially the same thresholds of instability in the case with convexification and without, due to the very low percentage of slackening, see $\mathcal{M}$. This fact is not surprising, since a longitudinal motion of the deck like a $\sin(\frac{\pi}{L}x)$ modifies the convexity of the cable only for very large

displacements, requiring a so large amount of energy that the threshold of instability is achieved before the appearance of slackening.

Quite different is the behavior of the modes from the 4^{th} onward, since in these cases we appreciate differences between two models, due to the strong percentage of slackening in the convexified case. We distinguish two tendencies respectively for the intermediate modes (4^{th}, 5^{th} and 6^{th}) and the higher modes. The thresholds of the intermediate modes reveal that the instability arises earlier for the model with inextensible hangers, so that the latter can be adopted in favor of safety. We point out that the 4^{th}, 5^{th} and 6^{th} modes were not seen the day of the collapse of the TNB; the witnesses recorded that, before the rise of the torsional instability, the bridge manifested longitudinal oscillations with 9 or 10 waves, involving the motion of higher longitudinal modes. For these modes the presence of the slackening puts down the thresholds of instability so that the assumption of rigid hangers is not in favor of safety. We underline that in these cases we see more instability despite the injection of energy is smaller; this behavior is peculiar of the hangers slackening that favors a greater transfer of energy between modes with respect to the case with inextensible hangers, see also [16]. The results in Table 2 highlight furthermore that the 9^{th} and 10^{th} longitudinal modes present the lowest torsional instability threshold in the case with slackening, confirming the real observations at the TNB collapse.

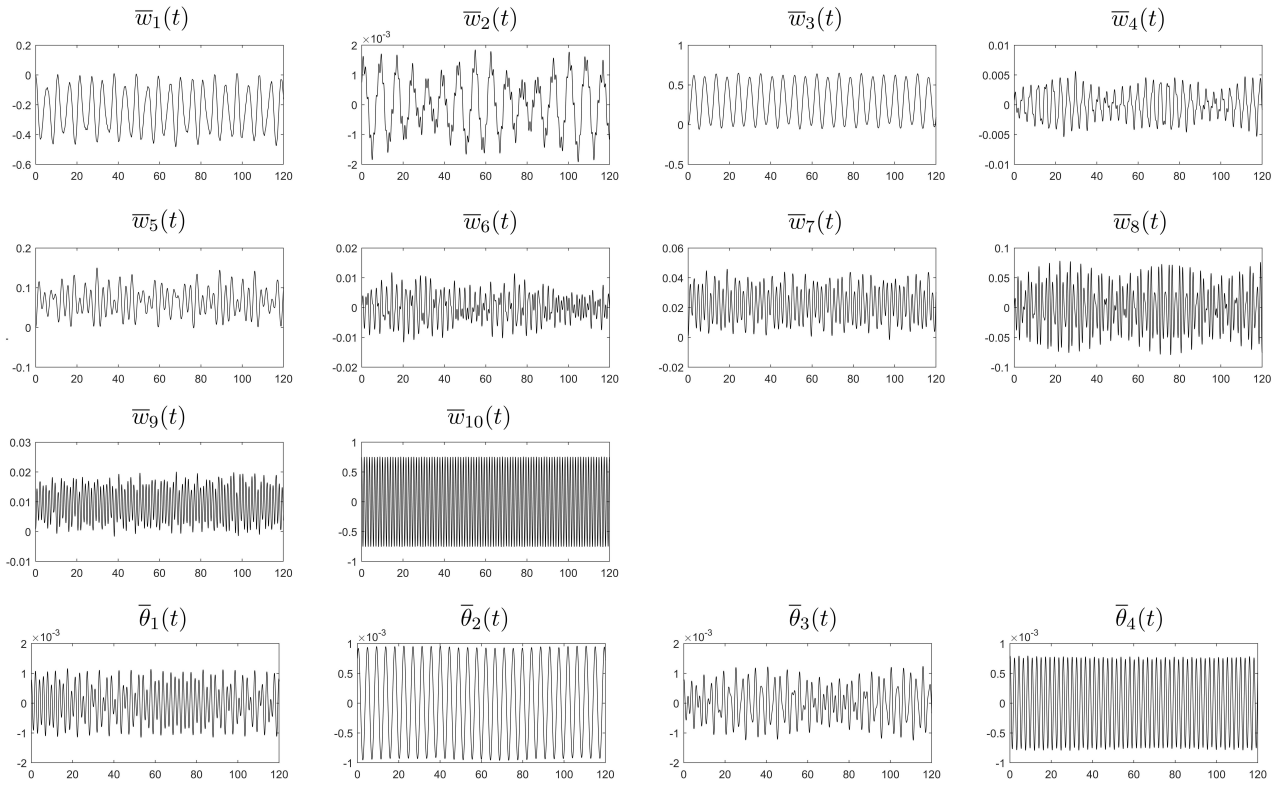

Figure 7: Plots of $\overline{w}_k(t)$ $(k = 1, \ldots, 10)$ in meters and $\overline{\theta}_k(t)$ $(k = 1, \ldots, 4)$ in radians on $[0, 120s]$ with $\overline{w}^0_{10}$=0.75m.

In Figure 7 we exhibit an example of stability obtained on the system with convexification, imposing $\overline{w}^0_{10}$ =0.75m; we record a very little exchange of energy between modes and, in general, the torsional modes oscillate around their initial amplitude, revealing a stable behavior. In this case some slack is present ($\mathcal{M}$ = 13.50%), while reducing further the initial amplitude would produce, as one can imagine, the total absence of slackening and a clear stable situation, see [17]; this happens for instance if $\overline{w}^0_9 \leq$0.60m and $\overline{w}^0_{10} \leq$0.55m.

For brevity in Figure 8 we present only the torsional modes related to the instability thresholds of

the 9^{th} and 10^{th} longitudinal modes, obtained respectively applying $\overline{w}_9^0$ =2.31m and $\overline{w}_{10}^0$ =2.65m. In general, when (5.2) is verified all the torsional modes begin to grow, but Figure 8 confirms that the 9^{th} and 10^{th} longitudinal modes are more prone to develop instability on the 2^{nd} torsional mode, since it attains the largest grow on $[0, 120s]$.

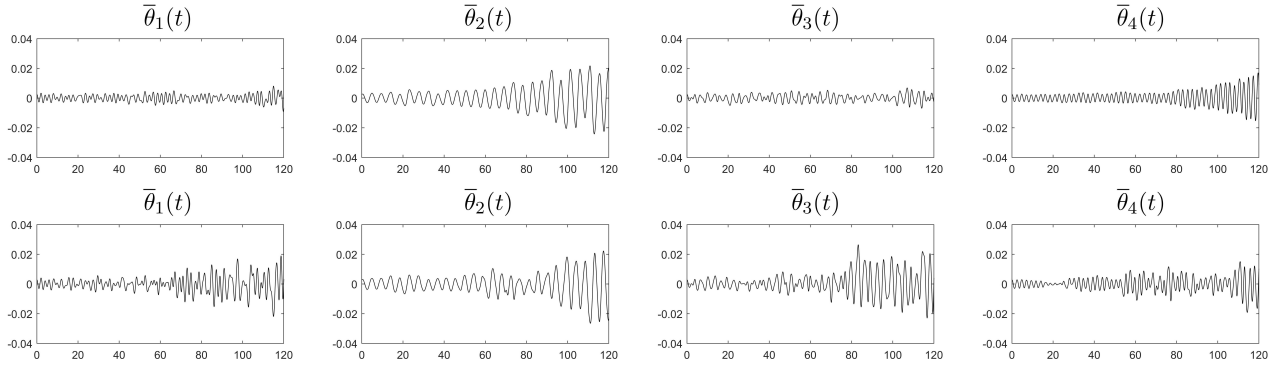

Figure 8: Plots of $\overline{\theta}_k(t)$ $(k = 1, \ldots, 4)$ in radians on $[0, 120s]$ with $\overline{w}_9^0$=2.31m (above) and $\overline{w}_{10}^0$=2.65m (below).

From Table 2 we also observe that the mean measure of the slackening $\mathcal{M}$ is increasing with respect to the energy introduced in the system, as physically one can expect. We now introduce a *mean measure of the hangers slackening* of each cable with respect to their position on $[0, L]$. We define it for the cable having vertical displacement $(w + \ell \sin\theta + y)^{**}$ as

$$\mathcal{S}^\alpha(x) := \frac{1}{m}\sum_{h=1}^{m} \chi_h^\alpha(x) \qquad \chi_h^\alpha(x) := \begin{cases} 1 & x \in \bigcup\limits_{i\in J_\alpha} K_\alpha^i, \\ 0 & x \in \overline{\mathcal{I}} \setminus \bigcup\limits_{i\in J_\alpha} K_\alpha^i, \end{cases} \tag{5.4}$$

in which $\chi_h^\alpha(x)$ is computed for every time step Δt_h; a similar relationship can be found for the other cable.

In Figure 9 we plot the function $\mathcal{S}^\alpha(x)$, defined in (5.4), representing the mean measure of the hangers slackening with respect to their position on $[0, L]$. As we can see in the stable situation ($\overline{w}_{10}^0$=0.75m, on the left) there is a clear trend of maximum slackening for the hangers corresponding to the points $x = \frac{L}{20} + \frac{L}{10}k$ with $k = 0, \ldots, 9$, i.e. the peaks of the function $\sin(\frac{10\pi}{L}x)$; indeed, in this case, the deck's motion follows sharply the 10^{th} longitudinal mode, excited through the initial conditions, see Figure 7. In Figure 9 we also show $\mathcal{S}^\alpha(x)$ for two unstable situations corresponding to $\overline{w}_9^0$=2.31m and $\overline{w}_{10}^0$=2.65m; we distinguish some peaks distinctive of the longitudinal modes excited, but, due to the transfer of energy to the other modes, $\mathcal{S}^\alpha(x)$ assumes shapes less clear. Similar plots can be found for the hangers related to the other main cable.

Our numerical results show that structures displaying only low modes of vibration may be treated assuming inextensible hangers; this simplification reduces the computational costs and gives safe instability thresholds. On the other hand, if the structure vibrates on higher modes, this assumption could give overestimated thresholds to the detriment of safety; in this case the slackening of the hangers plays an important role. This fact should be a warning for the designers of bridges that are able to exhibit, in realistic situations, large vibration frequencies.

6 Proofs of the results on the convexification

The proofs of the results of Sections 2.2 and 2.3 require some basic tools of convex analysis (see e.g. [15, 26]).

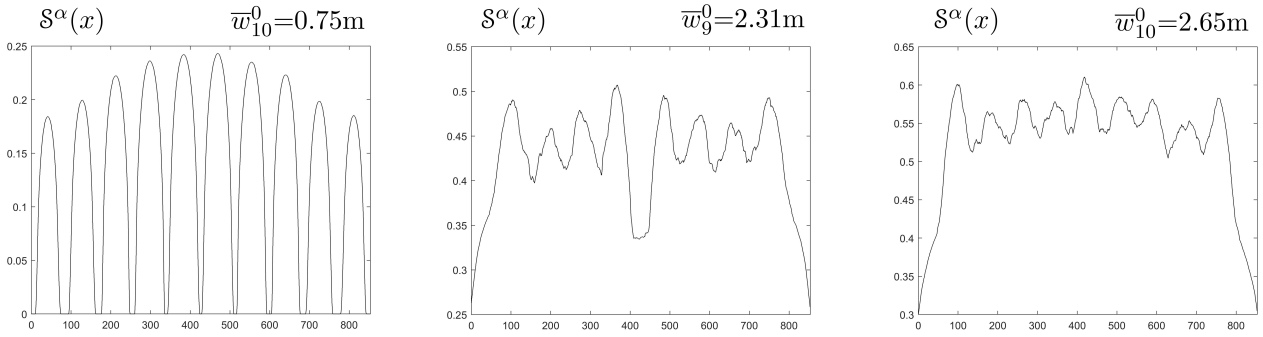

Figure 9: Plots of $\mathcal{S}^\alpha(x)$ on $[0, L]$, from the left in the cases $\overline{w}_{10}^0$=0.75m, $\overline{w}_9^0$=2.31m and $\overline{w}_{10}^0$=2.65m.

Given a closed convex set $E \subset \mathbb{R}^n$, a point $p \in \partial E$ is an extreme point of E if it is not contained in any open segment $]r, q[$ with $r, q \in \partial E$, whereas it is an exposed point of E if there exists a support hyperplane H to E with $H \cap E = \{p\}$. We denote by $\operatorname{extr} E$ and $\operatorname{expo} E$, respectively, the sets of extremal and exposed points of E, see Figure 10.

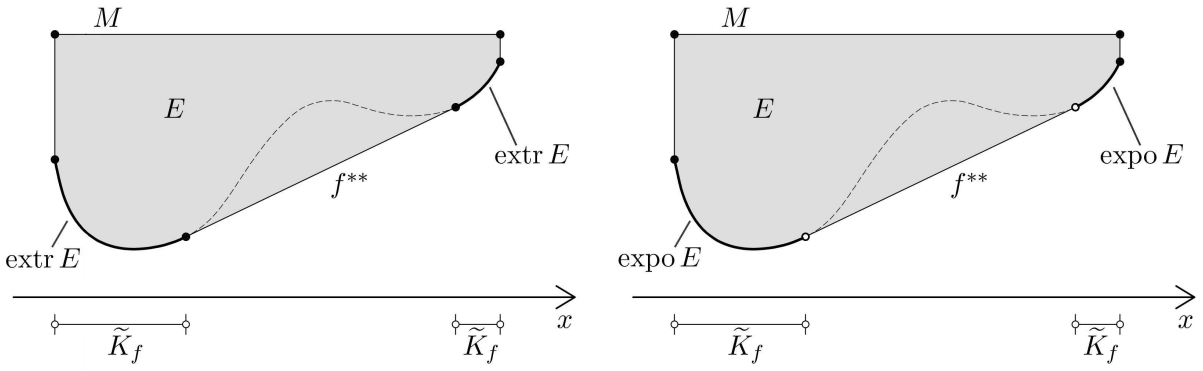

Figure 10: An example of $f^{**}(x)$ in which $\operatorname{extr} E$ and $\operatorname{expo} E$ are in evidence.

Clearly, $\operatorname{expo} E \subseteq \operatorname{extr} E$, but the inclusion may be strict even in dimension $n = 2$. If K is a compact convex set, then the Straszewicz's Theorem states that $\operatorname{extr} E \subseteq \overline{\operatorname{expo} E}$. Moreover, in dimension $n = 2$, the set $\operatorname{extr} E$ is closed (since every point $p \in \partial E \setminus \operatorname{extr} E$ is contained in a relatively open segment of ∂E).

Let us prove the following preliminary

Lemma 6.1. *Let $f \in C^1(\overline{\mathfrak{I}})$, and let $(f_n) \subset C^1(\overline{\mathfrak{I}})$ be a sequence converging uniformly to f. Then it holds:*

(a) If $x_0 \in \widetilde{K}_f$ and, for every $n \in \mathbb{N}$, $[a_n, b_n] \subset \overline{\mathfrak{I}}$, $\lambda_n \in [0, 1]$ satisfy

$$x_0 = (1 - \lambda_n)a_n + \lambda_n b_n, \qquad f_n^{**}(x_0) = (1 - \lambda_n)f_n(a_n) + \lambda_n f_n(b_n),$$

then $a_n, b_n \to x_0$.

(b) If, in addition, f satisfies assumption (2.9), i.e. $\overline{K_f} = \overline{\widetilde{K}_f}$, and (a_0, b_0) is one of the maximal intervals I^i where f^{**} is affine, then for every $n \in \mathbb{N}$ there exists a maximal interval (a_n, b_n) where f_n^{**} is affine such that $a_n \to a_0$, $b_n \to b_0$.

Proof. (a) Since x_0 is an exposed point of the epigraph of f^{**}, it holds

$$f(x) \geq f^{**}(x) > f(x_0) + f'(x_0)(x - x_0) \qquad \forall x \neq x_0.$$

Assume by contradiction that at least one of the sequences (a_n), (b_n) does not converge to x_0. Then there exists a subsequence (n_j) such that $a_{n_j} \to \overline{a}$, $b_{n_j} \to \overline{b}$, with $\overline{a} \leq x_0 \leq \overline{b}$ and $\overline{a} < \overline{b}$. Moreover, we clearly have $\lambda_{n_j} \to \lambda := (x_0 - \overline{a})/(\overline{b} - \overline{a})$. Hence,

$$f^{**}(x_0) = \lim_j f^{**}_{n_j}(x_0) = \lim_j (1 - \lambda_{n_j}) f_{n_j}(a_{n_j}) + \lambda_{n_j} f_{n_j}(b_{n_j}) = (1 - \lambda) f(\overline{a}) + \lambda f(\overline{b}) > f^{**}(x_0),$$

a contradiction.

(b) In view of (a), it is enough to prove that, if $x_0 \in (a_0, b_0)$, then $x_0 \notin K_{f_n}$ for n large enough.

Assume by contradiction that there exists a subsequence (n_j) such that $x_0 \in K_{f_{n_j}}$ for every j, i.e., $f_{n_j}(x_0) = f^{**}_{n_j}(x_0)$ for every j. Since, by assumption, $f > f^{**}$ on (a_0, b_0), one has

$$f(x_0) > f^{**}(x_0) = \lim_j f^{**}_{n_j}(x_0) = \lim_j f_{n_j}(x_0) = f(x_0),$$

a contradiction. □

Proof of Proposition 2.2. Let $M > \max_{[a,b]} f$, so that $E := \operatorname{epi} f^{**} \cap \{y \leq M\}$ is a compact convex subset of $\mathbb{R}^2$. Moreover, we have that

$$\{(x, f(x)) : \ x \in \widetilde{K}_f \cup \{a, b\}\} = \operatorname{expo} E \cap \{y < M\},$$

i.e., the set at left-hand side coincides with the set of exposed points of $\operatorname{epi} f^{**}$.

We introduce the notation

$$f_s := f + s\,\varphi, \quad f^{**}_s := (f_s)^{**}, \qquad s \in \mathbb{R}.$$

By the Dominated Convergence Theorem, Proposition 2.2 will be a consequence of the following pointwise convergences:

$$\lim_{s \to 0} \frac{f^{**}_s(x_0) - f^{**}(x_0)}{s} = \varphi(x_0) \qquad \text{if} \quad x_0 \in \widetilde{K}_f, \tag{6.1}$$

$$\lim_{s \to 0^{\pm}} \frac{f^{**}_s(x_0) - f^{**}(x_0)}{s} = \pm(\varphi_i^{\pm})^{**}(x_0) \qquad \text{if} \quad x_0 \in K^i, \ i \in J_C. \tag{6.2}$$

STEP 1. Proof of (6.1).

We have already observed that, if $x_0 \in \widetilde{K}_f$, then $f^{**}(x_0) = f(x_0)$ and $(x_0, f(x_0)) \in \operatorname{expo} E$.

Since $f \in C^1$, by definition of exposed point we have that

$$f(x) \geq f^{**}(x) > f(x_0) + f'(x_0)\,(x - x_0) =: h(x), \qquad \forall x \in [a, b], \ x \neq x_0.$$

For every $s \in \mathbb{R}$ let $a_s \in [a, x_0]$, $b_s \in [x_0, b]$, and $\lambda_s \in [0, 1]$ be such that

$$x_0 = (1 - \lambda_s) a_s + \lambda_s\, b_s, \qquad f^{**}_s(x_0) = (1 - \lambda_s) f_s(a_s) + \lambda_s\, f_s(b_s)\,. \tag{6.3}$$

Let us first prove that

$$\lim_{s \to 0^+} \frac{f^{**}_s(x_0) - f^{**}(x_0)}{s} = \varphi(x_0)\,. \tag{6.4}$$

Since

$$\frac{f^{**}_s(x_0) - f^{**}(x_0)}{s} \leq \frac{f_s(x_0) - f(x_0)}{s} = \varphi(x_0), \qquad \forall s > 0,$$

it follows that

$$\limsup_{s\to 0^+} \frac{f_s^{**}(x_0) - f^{**}(x_0)}{s} \le \varphi(x_0),$$

hence it remains to prove that

$$l := \liminf_{s\to 0^+} \frac{f_s^{**}(x_0) - f^{**}(x_0)}{s} \ge \varphi(x_0).$$

Let $s_n \searrow 0$ be a sequence such that

$$l = \lim_{n\to+\infty} \frac{f_{s_n}^{**}(x_0) - f^{**}(x_0)}{s_n}\,.$$

Using (6.3) it holds

$$\begin{aligned} \frac{f_{s_n}^{**}(x_0) - f^{**}(x_0)}{s_n} &= \frac{(1-\lambda_{s_n}) f_{s_n}(a_{s_n}) + \lambda_{s_n} f_{s_n}(b_{s_n}) - f(x_0)}{s_n} \\ &= \frac{(1-\lambda_{s_n}) f(a_{s_n}) + \lambda_{s_n} f(b_{s_n}) - f(x_0)}{s_n} + (1-\lambda_{s_n})\varphi(a_{s_n}) + \lambda_{s_n}\varphi(b_{s_n})\,. \end{aligned} \tag{6.5}$$

Since the sequence $\{f_{s_n}\}$ converges uniformly to f, by Lemma 6.1(i) it follows that $a_{s_n}, b_{s_n} \to x_0$, hence the right-hand side of (6.5) converges to a quantity greater than or equal to $\varphi(x_0)$, so that $l \ge \varphi(x_0)$ and (6.4) follows.

The computation of the limit (6.4) for $s \to 0^-$ can be done similarly, observing that the same inequalities as above hold with reversed signs. Hence, we conclude that (6.1) holds.

STEP 2. Proof of (6.2).

We shall prove (6.2) only for $s \to 0^+$, being the proof for $s \to 0^-$ entirely similar. Let $i \in J_C$ and let us denote

$$B := K^i \cap (K_f \cup \{a, b\}), \qquad A := K^i \setminus B.$$

Clearly, the set B is closed and contains both the endpoints of the interval K^i.

It is not restrictive to assume that $f^{**}(x) = 0$ for every $x \in K^i$, so that

$$f(x) = 0 \quad \forall x \in B, \qquad f(x) > 0 \quad \forall x \in A. \tag{6.6}$$

Let us extend the function φ_i^+ to $+\infty$ outside K^i. Since $\varphi \le \varphi_i^+$ and $(f + s\,\varphi_i^+)(x) = s\,\varphi_i^+(x)$ for every $x \in K^i$, we have that

$$f_s^{**}(x) = (f + s\,\varphi)^{**}(x) \le (f + s\,\varphi_i^+)^{**}(x) = s\,(\varphi_i^+)^{**}(x), \qquad \forall x \in K^i,$$

hence

$$\limsup_{s\to 0^+} \frac{f_s^{**}(x_0) - f^{**}(x_0)}{s} \le (\varphi_i^+)^{**}(x_0), \qquad \forall x_0 \in K^i.$$

Let $s_n \searrow 0$ be a sequence such that

$$l := \liminf_{s\to 0^+} \frac{f_s^{**}(x_0) - f^{**}(x_0)}{s} = \lim_{n\to+\infty} \frac{f_{s_n}^{**}(x_0) - f^{**}(x_0)}{s_n}\,,$$

and let $E_n := \operatorname{epi} f_{s_n}^{**} \cap \{y \le M\}$, $n \in \mathbb{N}$. By (6.6), for every $\varepsilon > 0$, there exists $N_\varepsilon \in \mathbb{N}$ such that, for $n \ge N_\varepsilon$, the extreme points of E_n are contained in $B + B_\varepsilon$, so that

$$K_{f_{s_n}} \cap K^i \subset B + B_\varepsilon \qquad \forall n \ge N_\varepsilon. \tag{6.7}$$

Let

$$\varphi_\epsilon(x) := \begin{cases} \varphi(x) & x \in B + B_\varepsilon, \\ +\infty & \text{otherwise,} \end{cases}$$

so that $\varphi_\epsilon(x) = \varphi_i^+(x)$ for every $x \in B$ and $\varphi_\epsilon \to \varphi_i^+$ pointwise in K_i. From the inclusion (6.7) it holds

$$f_{s_n}^{**}(x) = (f + s_n\,\varphi_\epsilon)^{**}(x), \qquad \forall x \in K^i,\ \forall n \geq N_\varepsilon,$$

so that

$$l = \lim_{n\to+\infty} \frac{f_{s_n}^{**}(x_0) - f^{**}(x_0)}{s_n} \geq \liminf_{n\to+\infty} \frac{(f + s_n\,\varphi_\epsilon)^{**}(x_0) - f^{**}(x_0)}{s_n} \geq \varphi_\varepsilon^{**}(x_0).$$

Finally, letting $\varepsilon \to 0$, we conclude that $l \geq (\varphi_i^+)^{**}(x_0)$, concluding the proof. □

Proof of Theorem 2.8. Since f satisfies assumption (2.9), we can use the same arguments of Step 1 in Proposition 2.2. We omit the details. □

Proof of Proposition 2.10. If $f \in C^0([a,b])$, it is easily seen that $Tf \in C^0([a,b])$, the functions F and F^{**} are in $C^1([a,b])$, and $F(a) = F^{**}(a) = 0$, $F(b) = F^{**}(b)$. As a consequence,

$$\int_a^b Tf(y)\,dy = \int_a^b f(y)\,dy \qquad \forall f \in C^0([a,b]). \tag{6.8}$$

In the following, we shall denote by K_F the contact set of F, defined by

$$K_F := \{x \in (a,b) :\ F(x) = F^{**}(x)\}.$$

We remark that $f = Tf$ on K_F. Moreover, we have the following characterization of K_F:

$$\begin{aligned} K_F &= \left\{x \in (a,b) :\ F(y) - F(x) - (y-x)F'(x) \geq 0,\ \forall y \in [a,b]\right\} \\ &= \left\{x \in (a,b) :\ \int_x^y [f(s) - f(x)]\,ds \geq 0,\ \forall y \in [a,b]\right\}. \end{aligned} \tag{6.9}$$

Let $f, g \in C^0([a,b])$ and let $F(x) := \int_a^x f(y)\,dy$, $G(x) := \int_a^x g(y)\,dy$, $x \in [a,b]$.
We claim that

$$f, g \in C^0([a,b]),\ f \leq g \qquad \Longrightarrow \qquad Tf \leq Tg. \tag{6.10}$$

Before proving this claim, let us observe that, from (6.8), (6.10) and Proposition 1 in [14], we can conclude that (2.14) holds.
It remains to prove that (6.10) holds. It will be convenient to perform a couple of reductions.

Reduction 1: it is not restrictive to assume that

$$f(a) = Tf(a), \quad f(b) = Tf(b), \qquad g(a) = Tg(a), \quad g(b) = Tg(b). \tag{6.11}$$

Namely, since

$$Tf(a) = \inf_{x\in(a,b]} \frac{F(x) - F(a)}{x - a} = \inf_{x\in(a,b]} \frac{1}{x-a} \int_a^x f(s)\,ds,$$

it is clear that $Tf(a) \leq f(a)$. If $Tf(a) < f(a)$, then there exists $\beta \in (a,b]$ such that (a,β) is a connected component of $(a,b) \setminus K_F$. Given $\varepsilon > 0$, let $c_\varepsilon := (1 + 1/\sqrt{2})\varepsilon$, and define the function

$$\varphi_\varepsilon(t) := \begin{cases} -1 + t/\varepsilon & \text{if } t \in [0, c_\varepsilon], \\ -1 + (2c_\varepsilon - t)/\varepsilon & \text{if } t \in [c_\varepsilon, 2c_\varepsilon - \varepsilon], \\ 0 & \text{otherwise,} \end{cases}$$

so that $\varphi_\varepsilon(0) = -1$ and $\int_0^{2c_\varepsilon - \varepsilon} \varphi_\varepsilon = 0$.

It is not difficult to show that, for $\varepsilon > 0$ small enough, the function $f_\varepsilon(x) := f(x) + [f(a) - Tf(a)]\,\varphi_\varepsilon(x-a)$ satisfies $Tf_\varepsilon = Tf$ and $Tf_\varepsilon(a) = f_\varepsilon(a)$. Moreover, we have $\|f_\varepsilon - f\|_1 \to 0$ as $\varepsilon \to 0$.

Similarly, we can modify f near b and the same can be done for the function g.

Reduction 2: it is not restrictive to assume that

$$f < g \qquad \text{in } [a,b]. \tag{6.12}$$

Namely, it is enough to check that $T(g+\varepsilon) = Tg + \varepsilon$.

So, let $f, g \in C([a,b])$ satisfy (6.11) and (6.12), and define

$$x_0 := \max\{x \in [a,b] :\ Tf(y) \le Tg(y)\ \forall y \in [a,x]\}.$$

Since $F \le G$, we have that $F^{**} \le G^{**}$ and hence $Tf(a) \le Tg(a)$. Moreover, by (6.11) and (6.12), we clearly have $x_0 > a$.

Assume by contradiction that $x_0 < b$, so that $Tf(x_0) = Tg(x_0)$, and let us consider the following cases.

Case 1: $x_0 \in K_F \cap K_G$. Hence,

$$Tf(x_0) = f(x_0) < g(x_0) = Tg(x_0),$$

in contradiction with $Tf(x_0) = Tg(x_0)$.

Case 2: $x_0 \in K_F$, $x_0 \notin K_G$. Let (α,β) be the maximal connected component of $(a,b)\setminus K_G$ containing x_0, so that Tg is constant on $[\alpha,\beta]$ and $g(\alpha) = Tg(\alpha)$, $g(\beta) = Tg(\beta)$. Here it is worth to remark that these equalities hold also in the case $\alpha = a$ or $\beta = b$ thanks to (6.11).

By the characterization (6.9) we have that:

$$x_0 \in K_F \quad \Longrightarrow \quad \int_{x_0}^{\beta} [f(s) - f(x_0)]\,ds \ge 0,$$

$$\beta \in K_G \text{ or } \beta = b \quad \Longrightarrow \quad \int_{x_0}^{\beta} [g(\beta) - g(s)]\,ds \ge 0,$$

so that

$$\int_{x_0}^{\beta} [g(\beta) - g(s) + f(s) - f(x_0)]\,ds \ge 0. \tag{6.13}$$

On the other hand $g(\beta) = Tg(\beta) = Tg(x_0)$ and $f(x_0) = Tf(x_0)$. Since $Tf(x_0) = Tg(x_0)$, we conclude that $g(\beta) = f(x_0)$, hence from (6.13) it holds

$$\int_{x_0}^{\beta} [f(s) - g(s)]\,ds \ge 0,$$

contradicting the assumption $f < g$.

Case 3: $x_0 \notin K_F$, $x_0 \in K_G$. We can reason as in the previous case, considering the connected component (α,β) of $(a,b)\setminus K_f$ containing x_0, and obtaining the inequality

$$\int_{\alpha}^{x_0} [g(x_0) - g(s) + f(s) - f(\alpha)]\,ds \ge 0.$$

Since, in this case, $g(x_0) = f(\alpha)$, we get again a contradiction with the assumption $f < g$.

Case 4: $x_0 \notin K_F$, $x_0 \notin K_G$. In this case Tf and Tg are locally constant in a neighborhood of x_0, again in contradiction with the definition of x_0. □

Proof of Proposition 2.11. We divide the proof into two steps.

STEP 1. If $f \in L^1(a,b)$, and $(f_n) \subset C^0([a,b])$ is a sequence converging to f in L^1, then

$$Tf_n \to Tf \quad \text{a.e.,} \quad \text{and} \quad \|Tf_n - Tf\|_1 \to 0.$$

Let $F(x) := \int_a^x f$, $F_n(x) := \int_a^x f_n$. We have that $F_n \to F$ uniformly in $[a,b]$, hence also $F_n^{**} \to F^{**}$ uniformly in $[a,b]$. (Proof: use the characterization $F^{**}(x) = \min\{(1-\lambda)F(x_0) + \lambda F(x_1) : \lambda \in [0,1],\ (1-\lambda)x_0 + \lambda x_1 = x\}$.) By Theorem 24.5 in [26] we deduce that $(F_n^{**})' \to (F^{**})'$ at every point of differentiability of F^{**}, i.e. almost everywhere in $[a,b]$. By definition of T, it follows that $Tf_n \to Tf$ almost everywhere in $[a,b]$.

The L^1 convergence of (Tf_n) to Tf follows from Proposition 2.10. Namely, from (2.14) we have that $\|Tf_n - Tf_m\|_1 \le \|f_n - f_m\|_1$, hence (Tf_n) is a Cauchy sequence in L^1 (and so it converges to its pointwise limit).

STEP 2. Completion of the proof.

Given $f, g \in L^1(a,b)$, let $(f_n), (g_n) \subset C^0([a,b])$ sequences converging in L^1 respectively to f and g. By Proposition 2.10, we have that $\|Tf_n - Tg_n\|_1 \le \|f_n - g_n\|_1$ for every n. Hence, by Step 1, passing to the limit as $n \to +\infty$ we obtain (2.15). □

Proof of Proposition 2.13. By (2.4) and (2.10) we have that

$$Tf = \begin{cases} \dfrac{F(b^i) - F(a^i)}{b^i - a^i} & x \in I^i,\ i \in J, \\ F'(x) & x \in K_F. \end{cases} \qquad (\mathcal{J}_F^\varphi)' = \begin{cases} \dfrac{\varphi(b^i) - \varphi(a^i)}{b^i - a^i} = \dfrac{\int_{a^i}^{b^i} \varphi' dx}{b^i - a^i} & x \in I^i,\ i \in J, \\ \varphi'(x) & x \in K_F, \end{cases}$$

and similarly for Tg and $(\mathcal{J}_G^\varphi)'$. Then we have the fundamental integral equivalence

$$\int_a^b [Tf\ (\mathcal{J}_F^\varphi)' - Tg\ (\mathcal{J}_G^\varphi)']dx = \int_a^b [Tf - Tg]\ \varphi' dx, \quad \forall \varphi \in C_c^\infty(\mathcal{I}) \tag{6.14}$$

so that the thesis is achieved by applying the Hölder inequality and Proposition 2.11. □

Proof of Proposition 2.14. i) Let us observe that

$$\int_a^b [\mathcal{H}(Tf)\ (\mathcal{J}_F^\varphi)' - \mathcal{H}(Tg)\ (\mathcal{J}_G^\varphi)']dx = \int_a^b [\mathcal{H}(Tf) - \mathcal{H}(Tg)]\ \varphi' dx, \quad \forall \varphi \in C_c^\infty(\mathcal{I})$$

then we proceed as in Proposition 2.13, considering the Lipschitz property of $\mathcal{H}$.

ii) We consider the equivalence

$$\begin{aligned} &\int_a^b [\mathcal{H}(Tf)\ (\mathcal{G}^{F,\psi})' - \mathcal{H}(Tg)\ (\mathcal{G}^{G,\psi})']dx = \int_a^b [\mathcal{H}(Tf)(\psi \cos F)' - \mathcal{H}(Tg)(\psi \cos G)']dx \\ &= \int_a^b [\mathcal{H}(Tf) - \mathcal{H}(Tg)](\psi \cos F)' dx + \int_a^b \mathcal{H}(Tg)\ (\psi \cos F - \psi \cos G)' dx \quad \forall \psi \in C_c^\infty(\mathcal{I}). \end{aligned} \tag{6.15}$$

Since $(\psi \cos F - \psi \cos G)' = \psi'(\cos F - \cos G) - \psi[(f-g)\sin F + g(\sin F - \sin G)]$, the thesis follows by the Lipschitzianity of the trigonometric functions and by proceeding as in the proofs above. □

Proof of Proposition 2.15. The functions $\mathcal{J}_n^\varphi$ are Lipschitz continuous, with

$$\|\mathcal{J}_n^\varphi\|_\infty \le \|\varphi\|_\infty, \qquad \|(\mathcal{J}_n^\varphi)'\|_\infty \le \|\varphi'\|_\infty.$$

Hence, by the Dominated Convergence Theorem, it is enough to show that $\mathcal{J}_n^\varphi \to \mathcal{J}^\varphi$ and $(\mathcal{J}_n^\varphi)' \to (\mathcal{J}^\varphi)'$ almost everywhere in $\mathcal{I}$.

The pointwise convergence of $\{\mathcal{J}_n^\varphi\}$ to $\mathcal{J}^\varphi$ is a direct consequence of Lemma 6.1.

To prove the a.e. convergence of $\{(\mathcal{J}_n^\varphi)'\}$ to $(\mathcal{J}^\varphi)'$, it will be convenient to distinguish between the two cases (a) and (b) in Lemma 6.1.

Let x_0 be as in case (a), and assume that all the function $\mathcal{J}_n^\varphi$ are differentiable at x_0 (this condition is satisfied at almost every point). For every n, if $x_0 \in K_{f_n}$ (i.e. $a_n = b_n$) then $(\mathcal{J}_n^\varphi)'(x_0) = \varphi'(x_0)$, otherwise there exists a point $x_n \in (a_n, b_n)$ such that

$$(\mathcal{J}_n^\varphi)'(x_0) = \frac{\varphi(b_n) - \varphi(a_n)}{b_n - a_n} = \varphi'(x_n).$$

Since $a_n, b_n \to x_0$, we finally get $(\mathcal{J}_n^\varphi)'(x_0) \to \varphi'(x_0) = (\mathcal{J}^\varphi)'(x_0)$.

Let x_0 be as in case (b). Then, for n large enough,

$$(\mathcal{J}_n^\varphi)'(x_0) = \frac{\varphi(b_n) - \varphi(a_n)}{b_n - a_n} \to \frac{\varphi(b_0) - \varphi(a_0)}{b_0 - a_0} = (\mathcal{J}^\varphi)'(x_0),$$

and the proof is complete. □

7 Proofs of existence and uniqueness results

To simplify the notations we define the functionals

$$\chi(u) := \frac{u'}{\sqrt{1 + (u')^2}}, \qquad \gamma(u) := \sqrt{1 + (u')^2} \tag{7.1}$$

and we state a preliminary

Lemma 7.1. *The functionals $\chi, \gamma : C^1[0, L] \to C^0[0, L]$ are locally Lipschitz continuous.*

Proof. Given $v, w \in C^1[0, L]$, we apply the Lagrange Theorem, so that there exists $\varrho := \varrho(x) \in \big(v', w'\big)$ such that

$$\big|\chi(v) - \chi(w))\big| = \frac{|v' - w'|}{\sqrt{(1 + \varrho^2)^3}} \le |v' - w'|, \qquad \big|\gamma(v) - \gamma(w))\big| = \frac{|\varrho||v' - w'|}{\sqrt{1 + \varrho^2}} \le |v' - w'|.$$

□

Proof of Theorem 4.2. Let $n \ge 1$ an integer. The local existence of a solution (w_n^k, θ_n^k) for all $k = 1, \dots, n$ and $t \ge 0$ depends on the regularity of the right hand side terms of (4.7). We introduce the vectors $W = [w_n^1, \dots, w_n^n]$, $\Theta = [\theta_n^1, \dots, \theta_n^n]$ and $e(x) = [e_1(x), \dots, e_n(x)]$ belonging to $\mathbb{R}^n$; we study the nonlinearities related to one cable, the other being similar.

If the functions

$$F_k(W, \Theta) := \big[H\overline{\xi} + \frac{AE_c}{L_c}\Gamma\big(W \cdot e + \ell \sin(\Theta \cdot e)\big] \int_0^L \chi\Big([W \cdot e + \ell \sin(\Theta \cdot e) + y]^{**}\Big)\, (\mathcal{J}_\alpha^{e_k})' dx,$$

$$G_k(W, \Theta) := \big[H\overline{\xi} + \frac{AE_c}{L_c}\Gamma\big(W \cdot e + \ell \sin(\Theta \cdot e)\big] \int_0^L \chi\Big([W \cdot e + \ell \sin(\Theta \cdot e) + y]^{**}\Big)\, (\mathcal{G}_\alpha^{\Theta \cdot e, e_k})' dx,$$

are locally Lipschitz continuous with respect to W and Θ for all $k = 1, \dots, n$, we have the existence and uniqueness of a solution of (4.7) on some interval $[0, t_n)$ with $t_n \in (0, T]$.

Thanks to Lemma 7.1, Proposition 2.14-i) and (3.3), for every compact subset $X \subset \mathbb{R}^n$ there exists $C_0 > 0$ such that, for every $W_1, W_2, \Theta_1, \Theta_2 \in X$ we have

$$\begin{aligned}
&\big|F_k(W_1,\Theta_1) - F_k(W_2,\Theta_2)\big| = \bigg|\big[H\overline{\xi} + \frac{AE_c}{L_c}\Gamma\big(W_1\cdot e + \ell\sin(\Theta_1\cdot e)\big)\big]\cdot \\
&\cdot \int_0^L \bigg[\chi\Big([W_1\cdot e + \ell\sin(\Theta_1\cdot e) + y]^{**}\Big)[(\mathcal{J}_\alpha^{e_k})_1]' - \chi\Big([W_2\cdot e + \ell\sin(\Theta_2\cdot e) + y]^{**}\Big)[(\mathcal{J}_\alpha^{e_k})_2]'\bigg]dx \\
&+ \frac{AE_c}{L_c}\bigg\{\int_0^L \bigg[\gamma\Big([W_1\cdot e + \ell\sin(\Theta_1\cdot e) + y]^{**}\Big) - \gamma\Big([W_2\cdot e + \ell\sin(\Theta_2\cdot e) + y]^{**}\Big)\bigg]dx\bigg\}\cdot \\
&\cdot \bigg\{\int_0^L \chi\Big([W_2\cdot e + \ell\sin(\Theta_2\cdot e) + y]^{**}\Big)[(\mathcal{J}_\alpha^{e_k})_2]'dx\bigg\}\bigg| \le C_0\|e_k'\|_\infty\big(|W_1 - W_2| + |\Theta_1 - \Theta_2|\big)\|e\|_{W^{1,1}},
\end{aligned} \tag{7.2}$$

so that $F_k(W,\Theta)$ is locally Lipschitz continuous for all $k = 1,\dots,n$. With some additional computations due to the presence of the trigonometric functions, see Proposition 2.14-ii), the same arguments can be applied to obtain the locally Lipschitz continuity of $G_k(W,\Theta)$.

Our purpose is now to find a uniform bound for the sequence (w_n,θ_n). We omit for the moment the spatial dependence of the approximated solutions. We test the first equation in (4.5) by $\dot w_n$, the second by $\dot\theta_n$ and we sum the two equations. Hence, we obtain

$$\begin{aligned}
&\frac{M}{2}\frac{d}{dt}\|\dot w_n\|_2^2 + \frac{EI}{2}\frac{d}{dt}\|w_n\|_{H^2}^2 + \frac{M\ell^2}{6}\frac{d}{dt}\|\dot\theta_n\|_2^2 + \frac{EJ}{2}\frac{d}{dt}\|\theta_n\|_{H^2}^2 + \frac{GK}{2}\frac{d}{dt}\|\theta_n\|_{H^1}^2 - \int_0^L Mg\dot w_n dx \\
&= -[H\overline{\xi} + \frac{AE_c}{L_c}\Gamma(w_n + \ell\sin\theta_n)]\int_0^L \frac{[(w_n + \ell\sin\theta_n + y)^{**}]_x}{\sqrt{1 + \{[(w_n + \ell\sin\theta_n + y)^{**}]_x\}^2}}(\mathcal{J}_\alpha^{\dot w_n} + \ell\mathcal{G}_\alpha^{\theta_n,\dot\theta_n})_x dx \\
&\quad - [H\overline{\xi} + \frac{AE_c}{L_c}\Gamma(w_n - \ell\sin\theta_n)]\int_0^L \frac{[(w_n - \ell\sin\theta_n + y)^{**}]_x}{\sqrt{1 + \{[(w_n - \ell\sin\theta_n + y)^{**}]_x\}^2}}(\mathcal{J}_\beta^{\dot w_n} - \ell\mathcal{G}_\beta^{\theta_n,\dot\theta_n})_x dx.
\end{aligned} \tag{7.3}$$

Let us define the energy of the system for the approximate solution (w_n,θ_n) as

$$\begin{aligned}
\mathcal{E}_n(t) :=& \frac{M}{2}\|\dot w_n\|_2^2 + \frac{EI}{2}\|w_n\|_{H^2}^2 + \frac{M\ell^2}{6}\|\dot\theta_n\|_2^2 + \frac{EJ}{2}\|\theta_n\|_{H^2}^2 + \frac{GK}{2}\|\theta_n\|_{H^1}^2 - Mg\int_0^L w_n dx \\
&+ H\overline{\xi}\int_0^L (\sqrt{1 + \{[(w_n + \ell\sin\theta_n + y)^{**}]_x\}^2} + \sqrt{1 + \{[(w_n - \ell\sin\theta_n + y)^{**}]_x\}^2})dx \\
&+ \frac{AE_c}{2L_c}\big([\Gamma(w_n + \ell\sin\theta_n)]^2 + [\Gamma(w_n - \ell\sin\theta_n)]^2\big).
\end{aligned}$$

Since we are in the finite dimensional setting it holds the assumption (2.9), so that we apply Corollary 2.3 and Theorem 2.8, finding the energy conservation. This is the point where we take advantage of the final dimensional nature of the problem. Hence from (7.3) we have $\dot{\mathcal{E}}_n(t) = 0$, that is

$$\begin{aligned}
&\mathcal{E}_n(t) = \mathcal{E}_n(0) = \frac{M}{2}\|w_n^1\|_2^2 + \frac{EI}{2}\|w_n^0\|_{H^2}^2 + \frac{M\ell^2}{6}\|\theta_n^1\|_2^2 + \frac{EJ}{2}\|\theta_n^0\|_{H^2}^2 + \frac{GK}{2}\|\theta_n^0\|_{H^1}^2 - Mg\int_0^L w_n^0 dx \\
&+ H\overline{\xi}\int_0^L (\sqrt{1 + \{[(w_n^0 + \ell\sin\theta_n^0 + y)^{**}]'\}^2} + \sqrt{1 + \{[(w_n^0 - \ell\sin\theta_n^0 + y)^{**}]'\}^2})dx \\
&+ \frac{AE_c}{2L_c}\bigg\{\bigg(\int_0^L [\sqrt{1 + \{[(w_n^0 + \ell\sin\theta_n^0 + y)^{**}]'\}^2}]dx - L_c\bigg)^2 + \bigg(\int_0^L [\sqrt{1 + \{[(w_n^0 - \ell\sin\theta_n^0 + y)^{**}]'\}^2}]dx - L_c\bigg)^2\bigg\}.
\end{aligned} \tag{7.4}$$

We recall the Poincaré inequality $\|w\|_2 \le \Lambda\|w\|_{H^2}$ for every $w \in H^2 \cap H_0^1$ ($\Lambda > 0$) and we observe that in $\mathcal{E}_n(t)$ only the gravitational term has undefined sign. In order to estimate this term we notice that for all $\varepsilon \in (0, \frac{1}{4}]$ we have

$$-\int_0^L w_n dx \ge -\int_0^L (1 + \varepsilon w_n^2)dx = -(L + \varepsilon\|w_n\|_2^2) \ge -(L + \varepsilon\Lambda^2\|w_n\|_{H^2}^2).$$

Choosing a sufficiently small $\varepsilon \in (0, \frac{1}{4}]$, we find $\eta > 0$ such that

$$\begin{aligned}\mathcal{E}_n(t) &\geq \frac{M}{2}\|\dot{w}_n\|_2^2 + \left(\frac{EI}{2} - Mg\Lambda\varepsilon\right)\|w_n\|_{H^2}^2 + \frac{M\ell^2}{6}\|\dot{\theta}_n\|_2^2 + \frac{EJ}{2}\|\theta_n\|_{H^2}^2 + \frac{GK}{2}\|\theta_n\|_{H^1}^2 \\ &\quad + H\bar{\xi}\int_0^L (\sqrt{1+\{[(w_n+\ell\sin\theta_n+y)^{**}]_x\}^2} + \sqrt{1+\{[(w_n-\ell\sin\theta_n+y)^{**}]_x\}^2})dx \\ &\quad + \frac{AE}{2L_c}\big([\Gamma(w_n+\ell\sin\theta_n)]^2 + [\Gamma(w_n-\ell\sin\theta_n)]^2\big) - MgL \\ &\geq \eta(\|\dot{w}_n\|_2^2 + \|w_n\|_{H^2}^2 + \|\dot{\theta}_n\|_2^2 + \|\theta_n\|_{H^2}^2 + \|\theta_n\|_{H^1}^2) - MgL.\end{aligned}$$

Then from (7.4) we infer that

$$\eta(\|\dot{w}_n\|_2^2 + \|w_n\|_{H^2}^2 + \|\dot{\theta}_n\|_2^2 + \|\theta_n\|_{H^2}^2 + \|\theta_n\|_{H^1}^2) \leq \mathcal{E}_n(0) + MgL \qquad \forall t \in [0, t_n) \text{ and } n \geq 1. \quad (7.5)$$

Thanks to (7.5) we obtain $t_n = T$, ensuring the global existence and uniqueness of the solution (w_n, θ_n) on $[0, T]$. Moreover, since the total energy of (4.5) is conserved in time, the solution cannot blow up in finite time and the global existence is obtained for an arbitrary $T > 0$, including $T = \infty$. □

Proof of Theorem 4.5. To simplify the notation we denote by $L^p(V)$ the space $L^p((0,T); V(0,L))$ for $1 \leq p \leq \infty$, by $Q = (0,T) \times (0,L)$ and by $C > 0$ all the generic positive constants. We observe that $\sup_n |\mathcal{E}_n(0)| + MgL < \infty$ is independent of n and t, since w_n^0 and θ_n^0 belong to $C^1[0,L]$, ensuring the convexification procedure in Section 2.1. Then from (7.5) we infer the boundedness of $\{w_n\}, \{\theta_n\}$ in $L^\infty(H^2)$ and of $\{\dot{w}_n\}, \{\dot{\theta}_n\}$ in $L^\infty(L^2)$, implying, up to a subsequence, the weak* convergence respectively to w, θ and to $\dot{w}$, $\dot{\theta}$ in the previous spaces. In particular from the boundedness of $\{w_n\}, \{\theta_n\}$ and $\{\dot{w}_n\}, \{\dot{\theta}_n\}$ we also have weak convergence respectively in $L^2(H^2)$ and $L^2(Q)$; then, due to the compact embedding $H^1(Q) \subset L^2(Q)$, we obtain the strong convergence

$$w_n \to w, \quad \theta_n \to \theta \qquad \text{in} \qquad L^2(Q), \quad (7.6)$$

from which $\sin\theta_n \to \sin\theta$ in $L^2(Q)$, since $\|\sin\theta_n - \sin\theta\|_{L^2(Q)} \leq \|\theta_n - \theta\|_{L^2(Q)} \to 0$ as $n \to \infty$ (similarly $\cos\theta_n \to \cos\theta$).

About the nonlocal term Γ, defined in (3.3), thanks to Lemma 7.1, Proposition 2.11, Hölder and Poincaré inequalities, we see that there exists $C > 0$ such that

$$|\Gamma(w_n \pm \ell\sin\theta_n) - \Gamma(w \pm \ell\sin\theta)| \leq (\|(w_n - w)_x\|_1 + \|\theta_n - \theta\|_{W^{1,1}}) \leq C(\|w_n - w\|_{L^\infty(H^2)} + \|\theta_n - \theta\|_{L^\infty(H^2)}) \to 0,$$

up to a subsequence, implying $\Gamma(w_n \pm \ell\sin\theta_n) \to \Gamma(w \pm \ell\sin\theta)$.

Let us now consider the functional χ, defined in (7.1), and note that $|\chi(u)| < 1$ for all $u \in H^2(0,L) \subset C^1[0,L]$. Then, we have that $\chi^2\big([w_n \pm \ell\sin\theta_n + y]^{**}\big) < 1$ and

$$\|\chi\big([w_n \pm \ell\sin\theta_n + y]^{**}\big)\|_{L^2(Q)}^2 = \int_0^T \int_0^L \frac{\{[(w_n \pm \ell\sin\theta_n + y)^{**}]_x\}^2}{1 + \{[(w_n \pm \ell\sin\theta_n + y)^{**}]_x\}^2} dxdt < LT.$$

Hence $\chi\big([w_n \pm \ell\sin\theta_n + y]^{**}\big)$ converges weakly, up to a subsequence, to $\chi\big([w \pm \ell\sin\theta + y]^{**}\big)$ in $L^2(Q)$ and it is possible to pass to the limit in the first equation in (4.5), since $\|(\mathcal{J}_\alpha^{e_k})'\|_\infty \leq \|e_k'\|_\infty$. To do the same for the second equation in (4.5) we use (6.15) and the bounds

$$\|\chi\big([w_n \pm \ell\sin\theta_n + y]^{**}\big)\cos\theta_n\|_{L^2(Q)}^2 < LT, \qquad \|\chi\big([w_n \pm \ell\sin\theta_n + y]^{**}\big)\theta_{nx}\sin\theta_n\|_{L^2(Q)}^2 \leq T\|\theta_n\|_{L^\infty(H^1)}^2,$$

which imply the weak convergence of these terms in $L^2(Q)$, up to a subsequence.

Next, for any $n \geq 1$ we put

$$w_n^0 := \sum_{k=1}^{n} (w^0, e_k)_2 \; e_k = \frac{L^4}{\pi^4} \sum_{k=1}^{n} \frac{(w^0, e_k)_{H^2}}{k^4} \; e_k,$$

$$\theta_n^0 := \sum_{k=1}^{n} (\theta^0, e_k)_2 \; e_k = \sum_{k=1}^{n} \left(EJ \frac{k^4 \pi^4}{L^4} + GK \frac{k^2 \pi^2}{L^2} \right)^{-1} [EJ(\theta^0, e_k)_{H^2} + GK(\theta^0, e_k)_{H^1}] \; e_k,$$

$$w_n^1 := \sum_{k=1}^{n} (w^1, e_k)_2 \; e_k, \qquad \theta_n^1 := \sum_{k=1}^{n} (\theta^1, e_k)_2 \; e_k,$$

so that

$$w_n^0 \to w^0, \;\; \theta_n^0 \to \theta^0 \;\text{ in }\; H^2, \qquad w_n^1 \to w^1, \;\; \theta_n^1 \to \theta^1 \;\text{ in }\; L^2$$

as $n \to \infty$.

Therefore we pass to the limit the problem (4.5)-(4.6), so that there exists an approximable solution of (4.2)-(4.3), $(w, \theta) \in X_T^2$ in the sense of Definition 4.4. □

8 Conclusions

A model inspired to the Melan equation [24] and to its variational formulation [21] was studied in [17], in which the main span of the suspension bridge was considered as a combined system of two perfectly flexible strings (the cables) linked to the deck through inextensible hangers. On the contrary a model with fixed cables and extensible hangers was considered in [16], focusing on the difficult choice of the slackening nonlinearities. In this paper, we proposed a model in which both the hangers and the cables are deformable. This was previously considered in [3] through a four DOF model, but here we have only focused on the vertical displacements and the torsional rotations of the deck, thereby dealing with a two DOF model. For the model considered in the present paper it appears out of reach to obtain a precise explanation of the origin of torsional instability in terms of Poincaré maps as in [2]. However, our numerical results still show the same qualitative phenomenon: after exceeding a certain energy threshold the system becomes unstable and sudden and violent torsional oscillations appear.

The analyisis of this new model for suspension bridges requires the study of the variation of an energy functional depending on the convexification of the involved functions. The computation of the Gateaux derivatives of the functional is quite involved and, apart of "spoiling" the action of the smooth test functions, it does not exist in some situations. After a full energy balance, in Section 4 we derived the weak form of the system of nonlinear nonlocal partial differential inclusions. This system is nonlinear due to the convexification, the geometric configuration of the cables and the rotation of the deck; moreover, we avoided the linearization based on smallness assumptions on the torsional angle of the deck. We included into the model not only the torsional effects on the deck due to de Saint Venant theory, but also more precise effects from the Vlasov theory.

The typical behavior of civil structures enabled us to consider approximable solutions as representative enough of our problem, thereby reducing to a system of ordinary differential equations, through the Galerkin procedure. We then proved existence of weak approximable solutions. This enabled us to study the problem numerically, considering 10 longitudinal modes interacting with 4 torsional modes and we found a threshold of torsional instability for each longitudinal mode excited. We compared these thresholds with the thresholds of instability of the correspondent model without convexification. Our numerical results show that, for structures displaying only low modes of vibration (e.g. 1^{st}, 2^{nd}, 3^{rd}), we may assume inextensible hangers, reducing the computational costs and obtaining safe instability thresholds. On the other hand, if the structure vibrates on higher modes (e.g. 9^{th}, 10^{th}) as the TNB,

this assumption may provide overestimated thresholds. Here the slackening of the hangers increases dangerously the torsional instability; this fact should be a warning for the designers of bridge structures, that are able to exhibit, in realistic situations, large vibration frequencies. Let us recall that the wind velocity determines the excited mode, see [1, pp.21-27] and that an explicit rule has been recently found in [8]. It turns out that the longitudinal modes that were torsionally unstable at the TNB were the 9^{th} and 10^{th}, precisely the ones for which we found lower thresholds of instability in the new model with convexification (that is, with hangers slackening).

References

[1] O.H. Ammann, T. von Kármán, G.B. Woodruff, *The failure of the Tacoma Narrows Bridge*, Federal Works Agency (1941).

[2] G. Arioli, F. Gazzola, *A new mathematical explanation of what triggered the catastrophic torsional mode of the Tacoma Narrows Bridge collapse*, Appl. Math. Modelling **39**, 901–912 (2015).

[3] G. Arioli, F. Gazzola, *On a nonlinear nonlocal hyperbolic system modeling suspension bridges*, Milan J. Math. **83**, 211–236 (2015).

[4] G. Arioli, F. Gazzola, *Torsional instability in suspension bridges: the Tacoma Narrows Bridge case*, Communications Nonlinear Sci. Numerical Simulation **42**, 342–357 (2017).

[5] J. P. Aubin, A. Cellina, *Differential inclusions. Set-valued maps and viability theory*, Springer-Verlag, Berlin, (1984).

[6] E. Berchio, F. Gazzola, *A qualitative explanation of the origin of torsional instability in suspension bridges*, Nonlinear Analysis TMA **121**, 54–72 (2015).

[7] F. Bleich, C.B. McCullough, R. Rosecrans, G.S. Vincent, *The mathematical theory of vibration in suspension bridges*, U.S. Dept. of Commerce, Bureau of Public Roads, Washington DC (1950).

[8] D. Bonheure, F. Gazzola, E. Moreira dos Santos, *Periodic solutions and torsional instability in a nonlinear nonlocal plate equation*, preprint (2018).

[9] D. Bucur, *Regularity of optimal convex shapes*, J. Convex Anal. **10**, no.2, 501–516 (2003).

[10] G. Buttazzo, V. Ferone, B. Kawohl, *Minumum problems over sets of concave functions and related questions*, Math. Nachr. **173**, 71–89 (1995).

[11] A. Capsoni, R. Ardito, A. Guerrieri, *Stability of dynamic response of suspension bridges*, J. Sound Vibration **393**, 285–307 (2017).

[12] A. Cellina, *A view on differential inclusions*, Rend. Semin. Mat. Univ. Politec. Torino **63**, 197–209 (2005).

[13] F.H. Clarke, *Optimization and nonsmooth analysis,* Jhon Wiley & Sons, New York (1983).

[14] M.G. Crandall, L. Tartar, *Some relations between nonexpansive and order preserving mappings*, Proc. Amer. Math. Soc. **78** , no. 3, 385–390 (1980).

[15] I. Ekeland, R. Temam, *Convex analysis and variational principles*, North-Holland, Amsterdam (1976).

[16] A. Falocchi, *Torsional instability in a nonlinear isolated model for suspension bridges with fixed cables and extensible hangers*, to appear in IMA Journal of Applied Mathematics.

[17] A. Falocchi, *Torsional instability and sensitivity analysis in a suspension bridge model related to the Melan equation*, Communications Nonlinear Sci. Numerical Simulation **67**, 60–75 (2019).

[18] M. Garrione, F. Gazzola, *Loss of energy concentration in nonlinear evolution beam equations*, J. Nonlinear Sci. **27**, 1789–1827 (2017).

[19] F. Gazzola, *Mathematical models for suspension bridges*, MS&A Vol. 15, Springer (2015).

[20] F. Gazzola, G. Sperone, *Thresholds for hanger slackening and cable shortening in the Melan equation for suspension bridges*, Nonlin. Anal. Real World Appl. **39**, 520–536 (2018).

[21] F. Gazzola, Y. Wang, R. Pavani, *Variational formulation of the Melan equation*, Math. Meth. Appl. Sci. **41**, 943–951 (2018).

[22] T. von Kármán, M.A. Biot, *Mathematical methods in engineering: an introduction to the mathematical treatment of engineering problems*, McGraw-Hill, New York (1940).

[23] J.L. Luco, J. Turmo, *Effect of hanger flexibility on dynamic response of suspension bridges*, J. Engineering Mechanics **136**, 1444–1459 (2010).

[24] J. Melan, *Theory of Arches and Suspension Bridges, Vol. 2*, Myron Clark Publ. Comp. London (1913).

[25] W. Podolny, *Cable-suspended bridges*, In: Structural steel designer's handbook: AISC, AASHTO, AISI, ASTM, AREMA and ASCE-07 Design standards, Ed. by R.L. Brockenbrough, F.S. Merritt, 5th edn., McGraw-Hill, New York (2011).

[26] R.T. Rockafellar, Convex Analysis, Princeton Univ. Press, Princeton, NJ, (1970).

[27] R.H. Scanlan, *The action of flexible bridges under wind, I: flutter theory, II: buffeting theory*, J. Sound and Vibration **60**, 187-199 & 201–211 (1978).

[28] F.C. Smith, G.S. Vincent, *Aerodynamic stability of suspension bridges: with special reference to the Tacoma Narrows Bridge, Part II: mathematical analysis.* Investigation conducted by the Structural Research Laboratory, University of Washington Press, Seattle, (1950).

[29] V.Z. Vlasov, *Thin-walled elastic bars*, (Russian) Fizmatgiz, Moscow (1959).

[30] V.A. Yakubovich, V.M. Starzhinskii, *Linear differential equations with periodic coefficients*, J. Wiley & Sons, New York (1975) (Russian original in Izdat. Nauka, Moscow, 1972).